Photosynthetic Production Determines Bottom Water Oxygen Variations in the Upwelling Coastal South China Sea Over Recent Decades

Xiaowei Zhu[1,2], Guodong Jia[3]*, Yuhang Tian[1,2], Aibin Mo[1,2], Weihai Xu[1,2], Li Miao[1,2], Shendong Xu[4] and Wen Yan[1,2,5]

[1]Southern Marine Science and Engineering Guangdong Laboratory (Guangzhou), Guangzhou, China, [2]Key Laboratory of Ocean and Marginal Sea Geology, South China Sea Institute of Oceanology, Chinese Academy of Sciences, Guangzhou, China, [3]State Key Laboratory of Marine Geology, Tongji University, Shanghai, China, [4]Guangxi Laboratory on the Study of Coral Reefs in the South China Sea, Coral Reef Research, Centre of China, School of Marine Sciences, Guangxi University, Nanning, China, [5]School of Marine Sciences, University of Chinese Academy of Sciences, Beijing, China

Dissolved oxygen (DO) in seawater is fundamental to marine ecosystem health. How DO in coastal upwelling areas responds to upwelling intensity under climate change is of particular interest and vital importance, because these productive regions account for a large fraction of global fishery production and marine biodiversity. The Yuedong upwelling (YDU) in the coastal northern South China Sea can be served as a study case to explore long-term responses of DO to upwelling and climate due to minor influence of riverine input. Here, bottom water DO conditions were recovered by sedimentary $C_{28}\Delta^{22}/\Delta^{5,22}$ ratios of steroids in three short cores, with lower ratio value indicating higher DO concentration. The ratio records showed oscillations in varying degrees and exhibited no clear trends before ~1980s, after which, however, there occurred a persistent decreasing trend or basically remained at lower values. Thus, inferred DO variations by the $C_{28}\Delta^{22}/\Delta^{5,22}$ ratio records are not compatible with regional YDU-involved physical processes under climate change, such as southwesterly wind-induced onshore advection of reduced-oxygenated source waters from outer shelf and oceanic warming that would rather lead to less oxygenation in bottom waters in recent decades. Intriguingly, the alcohol records of n-$C_{20:1}/C_{28}\Delta^{5,22}$ and br-$C_{15}/C_{28}\Delta^{5,22}$ ratios, indicative of the relative strengths between biogeochemical oxygen consumption (i.e., by zooplankton and microbes) and photosynthetic oxygen production (i.e., by phytoplankton), changed almost in parallel with the $C_{28}\Delta^{22}/\Delta^{5,22}$ records in three cores. Accordingly, we propose that net photosynthetic oxygen production outweighs source water– and warming-induced increasing deoxygenation in the study area. This study may suggest an important biogeochemical mechanism in determining bottom water DO dynamics in shallow coastal upwelling regions with minor contribution of riverine input.

Keywords: bottom water oxygen variation, ratios of 5a-stanols to D5-sterols, alcohol biomarkers, physical-biogeochemical processes, Yuedong upwelling

INTRODUCTION

The fate of dissolved oxygen (DO) in seawater has attracted increasing attentions from multi-disciplines, owing to its vital role in ecological, biological, and geochemical dynamics in marine environments (Diaz and Rosenberg, 2008; Breitburg et al., 2009; Breitburg et al., 2018; Levin and Breitburg, 2015; Watson, 2016; Schmidtko et al., 2017; Fennel and Testa, 2019). The inventory of oceanic DO is determined by the balance between its primary sources (i.e., photosynthetic production, air–sea gas exchange, and physical oxygen supply) and sinks (i.e., aerobic respiration and consumption, oxidation of reduced chemical species, and physical oxygen export) (Breitburg et al., 2018; Fennel and Testa, 2019). Over recent decades, various investigations based on time-series observations, numerical models, and geological records have been carried out to understand the physical-biogeochemical processes controlling the spatiotemporal distributions of low-oxygen (i.e., hypoxic and anoxic) conditions within the global ocean (e.g., Breitburg et al., 2018; Fennel and Testa, 2019, and references therein).

Generally, the occurrence of oxygen-deficiency in estuarine and river-dominated shelf regions is mainly attributed to the significant feedback of freshwater discharge and anthropogenic input, whereas the coastal upwelling areas without direct riverine and anthropogenic impacts experience low-oxygen conditions mostly due to supplies of oxygen-poor and nutrient-rich source waters at times of upwelling (Breitburg et al., 2018; Fennel and Testa, 2019). Long-term links between DO condition and upwelling intensity have been evidenced by sedimentary records of nitrogen isotope from the northeastern tropical Pacific margin, showing enhanced oxygenation in response to weakened wind-induced upwelling since 1850 (Deutsch et al., 2014). However, different relationships between DO and upwelling have been documented in other upwelling regions; e.g., overall enhanced oxygenation (Cardich et al., 2019) is observed in response to strengthened upwelling off Peru since 1860 (Gutierrez et al., 2011). These occurrences likely indicate that the proposed negative impact of upwelling activity on DO condition may be too simplistic, especially in terms of long-term (i.e., decadal and centurial scales) relationships. Besides, close links between upwelling-favorable wind and climate change proposed previously (Bakun, 1990) have been recently evidenced by observations, models, and records in many upwelling regions (Gutierrez et al., 2011; Sydeman et al., 2014; Wang et al., 2015), showing strengthened wind-induced upwelling in response to climatic warming. This scenario may further complicate long-term responses of DO condition to upwelling variation and climate change; however, this issue has not been investigated in upwelling regions in the coastal northern South China Sea (SCS) (Hu and Wang, 2016), including the Yuedong upwelling (YDU).

Recently, sedimentary records of long-chain diols in the YDU area revealed increasing trends in the upwelling intensity and annual mean sea surface temperature (SST) over recent decades (Zhu et al., 2018), supporting previous studies showing close links between upwelling intensification and climatic warming (Bakun, 1990; Gutierrez et al., 2011; Sydeman et al., 2014; Wang et al.,

2015). Long-chain diol records also demonstrated insignificant or indirect input from the Pearl River (Zhu et al., 2018), making the YDU as an ideal spot to explore long-term responses of DO variability to upwelling and climate. However, as available DO records are lacking in the YDU region, how DO responds to enhanced upwelling and increased SST remains unclear. This issue is relevant to fishery production, marine biodiversity, and ecosystem health over time so that proper proxies are essential to reconstruct long-term DO variations in the YDU area to fill in this gap.

Over the past few decades, an increasing number of DO-related proxies based on biomarkers, elements (i.e., molybdenum and uranium), and foraminifer (i.e., *Bulimina marginata* and *Quinqueloculina* spp.) have been proposed and applied to reconstruct paleo-DO or paleo-redox conditions (e.g., Nakakuni et al., 2017; Nakakuni et al., 2018; Li et al., 2018; Naafs et al., 2019; Jacobel et al., 2020; Wakeham, 2020, and references therein). Among the biomarker-derived redox proxies, the 5α-stanol/Δ^5-sterol ratios are widely used because eukaryote-derived Δ^5-sterols are ubiquitous in aquatic environments and can be anaerobically transformed to 5α-stanol counterparts without aerobic re-conversion (e.g., Gaskell and Eglinton, 1975; Wakeham, 1989; Wakeham, 2020; Berndmeyer et al., 2014; Nakakuni et al., 2017, 2018). Some other processes, such as *in vivo* production of 5α-stanols and preferential degradation of Δ^5-sterols may also modulate the 5α-stanol/Δ^5-sterol ratios and confound their applicability to reflect redox processes (e.g., Nishimura and Koyama, 1977; Wakeham, 1989; Arzayus and Canuel, 2004; Bogus et al., 2012). Therefore, before applying the 5α-stanol/Δ^5-sterol ratios to infer redox variations, their suitability as such an approach should be examined. Here, the 5α-stanol/Δ^5-sterol ratios were applied for the first time to elucidate their ability to reconstruct historical redox condition in the YDU area and further to explore the responses of DO dynamics to climate-forced YDU processes over recent decades.

Origin of Common Alcohols in Marine Environments and Factors Regulating the 5α-Stanol/Δ^5-Sterol Ratios

Generally, short-chain ($C_{14–18}$; the sum of C_{14}, C_{16} and C_{18}) *n*-alcohols are primarily derived from marine organisms and long-chain ($C_{26–30}$; the sum of C_{26}, C_{28} and C_{30}) *n*-alcohols are mainly produced by terrestrial vascular plants (e.g., Mudge and Norris, 1997; Treignier et al., 2006; Hu et al., 2009; Strong et al., 2012; Strong et al., 2013; Guo et al., 2019). The middle-chain unsaturated *n*-alcohols (i.e., *n*-$C_{20:1}$) are typically diagnostic biomarkers for copepods (Kattner and Krause, 1989) and short-chain branched alcohols (i.e., *br*-C_{15}; the sum of *iso*- and *anteiso*-C_{15}) are ubiquitous in marine environments produced by certain microbes (Mudge and Norris, 1997; Treignier et al., 2006; Huang et al., 2013; Yang et al., 2014; Naafs et al., 2019). The odd/even ratio of short-chain *n*-alcohols (i.e., $C_{15–17}/C_{16–20}$; the sum of C_{15} and C_{17}/the sum of C_{16}, C_{18} and C_{20}) indicates the degree of microbial alternation and is a rough measure of microbial activity (Treignier et al., 2006).

The C_{27-29} sterols have diverse and ecologically widespread sources, including aquatic plankton (i.e., phytoplankton and zooplankton) and terrestrial plants (Volkman, 1986; Volkman, 2003; Volkman et al., 1998; Rampen et al., 2010). Generally, zooplankton is the major biological precursor for C_{27} sterols, whereas C_{28} and C_{29} sterols appear to be particularly abundant in phytoplankton and terrestrial plants, respectively. However, a comprehensive study on 106 marine diatom species reveals that C_{27-29} sterols are all present with $C_{28}\Delta^{5,24(28)}$ being the most common component, followed by $C_{27}\Delta^5$, $C_{28}\Delta^5$, $C_{29}\Delta^5$, and $C_{28}\Delta^{5,22}$ (Rampen et al., 2010); nevertheless, none of these sterols can be used as an unambiguous diatom biomarker due to their wide occurrence in other algae (Volkman, 2003).

The 5α-stanols are generally derived from the anaerobic reduction of their Δ^5-sterol counterparts (e.g., Gaskell and Eglinton, 1975; Wakeham, 1989, 2020; Berndmeyer et al., 2014; Nakakuni et al., 2017; Nakakuni et al., 2018). The particulate matter studies at various depths of the water column from different marine settings revealed that the extent of conversion of Δ^5-sterols to 5α-stanol counterparts varies with water-column redox potential (Wakeham, 1989; Wakeham, 2020; Wakeham et al., 2007; Berndmeyer et al., 2014). Generally, little 5α-stanol generation occurs under oxic conditions, yielding low 5α-stanol/Δ^5-sterol ratios, whereas substantial conversion of Δ^5-sterols occurs in anoxic environments, resulting in high 5α-stanol/Δ^5-sterol ratios. However, the 5α-stanol/Δ^5-sterol ratios can also be regulated by direct biogenic input of 5α-stanols and/or preferential degradation of Δ^5-sterols relative to 5α-stanols (e.g., Nishimura and Koyama, 1977; Wakeham, 1989; Arzayus and Canuel, 2004; Bogus et al., 2012).

The occurrence of 5α-stanols has been reported in some species of marine organisms, such as diatoms (e.g., *Thalassionema nitzschioide* and *Skeletonema costatum*; Barrett et al., 1995; Rampen et al., 2010), dinoflagellates (e.g., *Scrippsiella* sp. and *Gymnodinium sanguineum*; Mansour et al., 1999), microalgae (e.g., *Pavlova* sp.; Volkman et al., 1990), and zooplankton (e.g., *Themisto gaudichaudi*; Nelson et al., 2000; Nelson et al., 2001). For example, *T. nitzschioide* and *S. costatum* produce a minute fraction (<11%) of 5α-stanols, such as $C_{27}\Delta^{22}$ and $C_{28}\Delta^{24(28)}$, respectively (Barrett et al., 1995; Rampen et al., 2010), and *Scrippsiella* sp. and *G. sanguineum* produce high fractional abundances of $C_{27}\Delta^0$ (24.3%) and $C_{28}\Delta^{22}$ (31.7%), respectively (Mansour et al., 1999). Recently, comprehensive investigations on a series of C_{26-29} 5α-stanol/Δ^5-sterol ratios in sediment cores demonstrated that some ratio pairs are not applicable to trace historical redox processes because of the interference of *in vivo* produced 5α-stanols by some organisms (Nakakuni et al., 2017; Nakakuni et al., 2018).

The preferential degradation of Δ^5-sterols relative to their 5α-stanol counterparts may also confound the 5α-stanol/Δ^5-sterol ratios to reflect anaerobic conversion processes (e.g., Arzayus and Canuel, 2004; Bogus et al., 2012). The higher rate of degradation than hydrogenation of Δ^5-sterols has been proposed to explain higher 5α-stanol/Δ^5-sterol ratios in sediments from the York River estuary (Arzayus and Canuel, 2004). This is followed by a subsequent study on surface sediments in a cross-shelf transect offshore the Pakistan continental margin, suggesting that the increasing trend in the $C_{27}\Delta^0/\Delta^5$ ratio is attributable to the faster degradation of $C_{27}\Delta^5$ compared with that of $C_{27}\Delta^0$ (Bogus et al., 2012).

MATERIALS AND METHODS

Study Area

The YDU, located in the inshore area from Hong Kong to the Nanri Islands (**Figure 1**), is a common phenomenon with a large spatial extent occurring in summer, leading to colder SST and higher salinity and nutrients than surrounding waters (Jing et al., 2011; Hu and Wang, 2016). The local southwesterly wind stress is one of the most important dynamical factors to induce the coastal YDU with apparent inter-annual variability (Jing et al., 2011; Hu and Wang, 2016). Recently, sedimentary records of long-chain diol index (LDI) and diol index 2 (DI-2), which are respective indicators for annual mean SST and southwesterly wind-induced upwelling intensity in the YDU area, revealed increasing warming and enhancing upwelling over recent decades (Zhu et al., 2018).
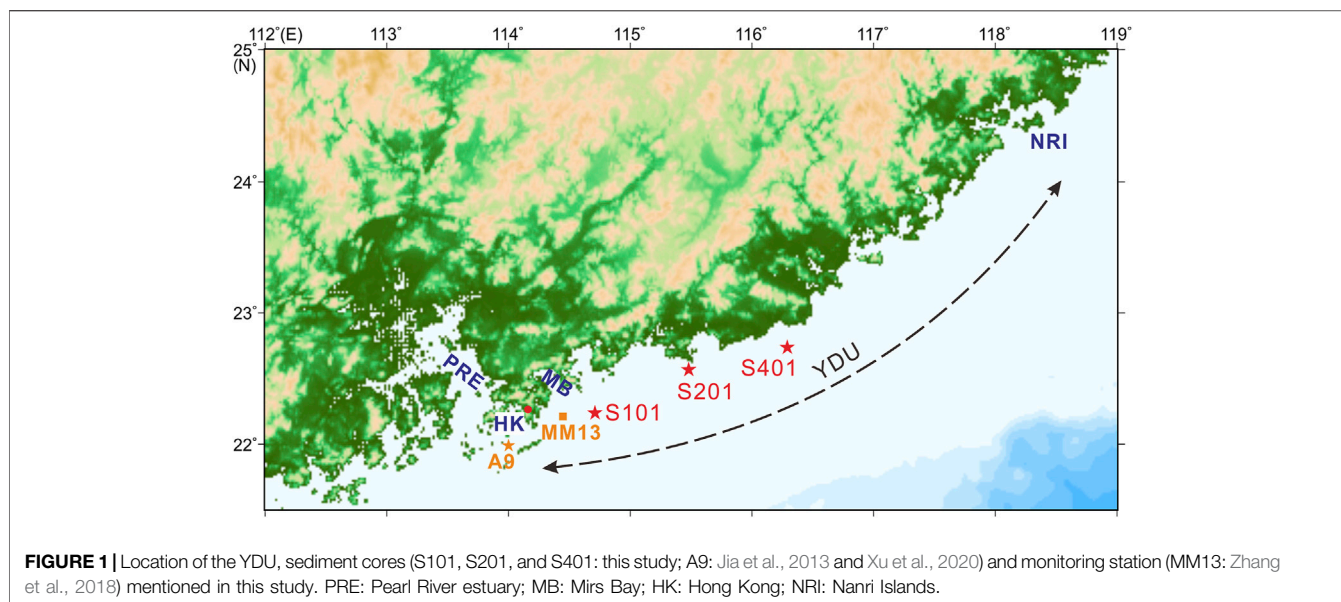
To the west of YDU is the Pearl River estuary (PRE; **Figure 1**), receiving discharges from the subtropical Pearl River. The river is the second largest river in China in terms of discharge, 80% of which occurs during the wet season (April to September). After being poured out of the estuary, the Pearl River plume swings seasonally (Dong et al., 2004; Su, 2004); it generally turns toward the west during the dry winter due to northeasterly winds and Coriolis effect and extends offshore toward south and southeast during wet summer under southwesterly winds when the Pearl River discharge reaches its maximum.

Sample Collection

In this work, three short box cores (**Figure 1**; **Table 1**) at the margin of the YDU were studied. They were collected in 2009 during the China Ocean Carbon (CHOICE-C) Cruise I onboard the *Dongfanghong II*. The core surfaces were well preserved upon collection, as demonstrated by the fairly clear water above the sediment surface in the box corers. After the overlying water being siphoned out, core barrels were pushed into each box to collect sub-cores. Sediment in the sub-cores was then (usually within an hour) extruded onboard using a hydraulic jack, and sectioned at 2-cm intervals. The sectioned samples were sealed in plastic jars, then frozen until they were freeze-dried at −50°C in the laboratory, and grounded with an agate mortar and pestle for further analyses and tests. The chronology of the cores has been determined by the ^{210}Pb method and reported by Zhu et al. (2018). **Table 1** shows the dating results and other information of the three cores.

Lipid Extraction, Separation and Measurement

The core sediments have been reported for long-chain diols and the detailed experiments for lipid extraction and separation can be found in the work of Zhu et al. (2018). Briefly, freeze-dried and powdered sediments were extracted ultrasonically with MeOH, dichloromethane (DCM)/MeOH (1:1, v/v), and DCM, and all

FIGURE 1 | Location of the YDU, sediment cores (S101, S201, and S401: this study; A9: Jia et al., 2013 and Xu et al., 2020) and monitoring station (MM13: Zhang et al., 2018) mentioned in this study. PRE: Pearl River estuary; MB: Mirs Bay; HK: Hong Kong; NRI: Nanri Islands.

TABLE 1 | Information of the three sediment cores.

	S101	S201	S401
Location			
Latitude (°N)	22.25	22.58	22.75
Longitude (°E)	114.71	115.48	116.29
Water depth (m)	35	31	24
Core length (cm)	40	40	24
Dating model			
MAR[a] (g/cm²/yr)	0.51	0.63	0.37
Time span (yr)	1941–2008	1965–2009	1930–2007
MTR[b] per 2 cm interval (yr)	3.6	2.3	7.1
MSR[c] (cm/yr)	0.57	0.85	0.28

[a]Mass accumulation rate.
[b]Mean temporal resolution.
[c]Mean sedimentation rate.

extracts were combined after centrifugation. Following saponification with KOH/MeOH and extraction into hexane, the neutral lipids were purified using silica gel chromatography by elution with DCM/n-hexane (4:1, v/v) and DCM/MeOH (2:1, v/v), respectively. The latter fraction containing alcohols was converted to trimethylsilyl derivatives with bis(trimethylsilyl)trifluoroacetamide (BSTFA) at 60°C for 2 h before gas chromatography–mass spectrometry (GC–MS) analyses.

GC–MS analysis was performed at the State Key Laboratory of Organic Geochemistry, Guangzhou Institute of Geochemistry, Chinese Academy of Sciences, with a Thermo Scientific Trace gas chromatograph coupled to a Thermo Scientific DSQ II mass spectrometer. Separation was achieved with a 60 m × 0.32 mm i.d., fused silica column (J and W DB-5) coated with a 0.25-µm film thickness. The oven temperature was programmed from 80°C (held 2 min) to 220°C at 6°C/min, then to 290°C (held 5 min) at 8°C/min, and at last to 315°C (held 25 min) at 2°C/min. Identification and quantification of alcohol compounds,

including n-alcohols, br-alcohols, sterols, and stanols, were based on their characteristic mass fragments, i.e., m/z 103 for n- and br-alcohols, 255 for Δ^5-and $\Delta^{5,22}$-sterols, 257 for Δ^{22}-sterols, and 215 for 5α-stanols (Huang et al., 2013; Yang et al., 2014; Nakakuni et al., 2017; Nakakuni et al., 2018).

Further, an approach proposed by Nakakuni et al. (2017); Nakakuni et al. (2018) was applied to determine the accuracy of the analytical 5α-stanol/Δ^5-sterol ratio results, especially the $C_{27}\Delta^{22}/\Delta^{5,22}$, $C_{27}\Delta^0/\Delta^5$, and $C_{28}\Delta^{22}/\Delta^{5,22}$ ratio pairs used in this study (see below). Four samples from cores S101 (2–4 cm and 22–24 cm) and S201 (0–2 cm and 22–24 cm) were measured replicated for quality control, because both cores with relatively low or even unquantifiable contents of Δ^5-sterols (this scenario can be seen roughly in mass spectrogram) were particularly susceptible to large deviations caused by pronounced background noise. Estimated values of relative standard deviation of the three ratio pairs in the four samples (2–4 cm and 22–24 cm in S101, and 0–2 cm and 22–24 cm in S201) ranged from 4% to 10%, similar to those (<10%) reported by Nakakuni et al. (2017); Nakakuni et al. (2018), implying high precision of the analytical results in the present study.

Degradation-Corrected Downcore Sterol Concentration

Using an approach similar to (Middelburg, 1989) power model, log-log plots of degradation rate constant (k) vs. time since deposition (t) were proposed by Canuel and Martens (1996) to evaluate the influence of post-diagenesis on downcore sterol concentration according to the following equation:

$$\log k = -1.12 \times \log t - 0.065, \text{ or } k = 0.86 \times t^{-1.12} \quad (1)$$

Further, given a known apparent initial age (a_0), the sterols$_{corr}$ (the initial sterols at the sediment surface before
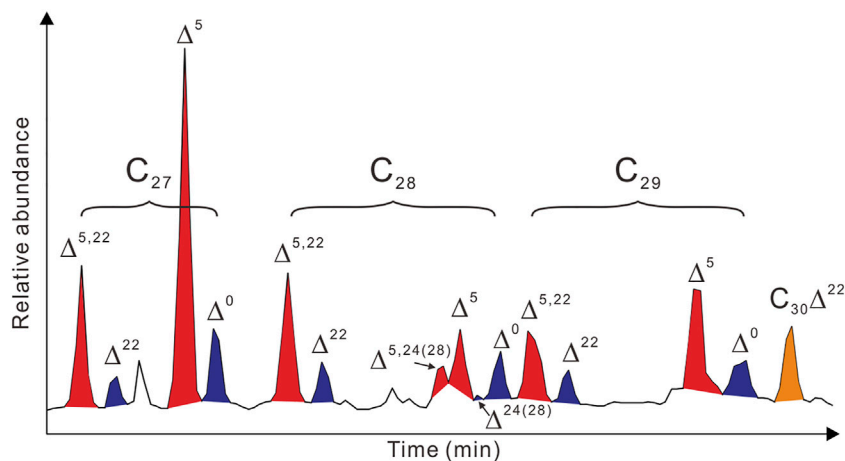
FIGURE 2 | Partial total ion chromatogram (TIC) of the alcohol fraction in core S401 sediments. Most of the sterols and stanols with abbreviation are labeled in the figure. The systematic and trivial names of each compound are present in **Table 2**; more detailed information can be found in published studies (e.g., Rampen et al., 2010; Nakakuni et al., 2017; Nakakuni et al., 2018).

TABLE 2 | Sterol and stanol compounds identified in core S401 (see **Figure 2** for TIC). Detailed information (i.e., structure, nomenclature, and source) of individual compounds can be found in, e.g., the works of Rampen et al. (2010) and Nakakuni et al. (2017, 2018).

Abbreviation	Systematic name	Trivial name
$C_{26}\Delta^{5,22}$	24-norcholesta-5,22-dien-3β-ol	24-Nordehydrocholesterol
$C_{26}\Delta^{22}$	24-nor-5α-cholest-22-en-3β-ol	24-Nordehydrocholestanol
$C_{27}\Delta^{5,22}$	cholesta-5,22-dien-3β-ol	22-Dehydrocholesterol
$C_{27}\Delta^{22}$	5α-cholest-22-en-3β-ol	22-Dehydrocholestanol
$C_{27}\Delta^{5}$	cholest-5-en-3β-ol	Cholesterol
$C_{27}\Delta^{0}$	5α-cholestan-3β-ol	Cholestanol
$C_{28}\Delta^{5,22}$	24-methylcholesta-5,22-dien-3β-ol	Brassicasterol
$C_{28}\Delta^{22}$	24-methyl-5α-cholesta-22-en-3β-ol	Brassicastanol
$C_{28}\Delta^{5,24(28)}$	24-methylcholesta-5,24(28)-dien-3β-ol	
$C_{28}\Delta^{5}$	24-methylcholest-5-en-3β-ol	Campesterol
$C_{28}\Delta^{24(28)}$	24-methyl-5α-cholesta-24(28)-en-3β-ol	
$C_{28}\Delta^{0}$	24-methyl-5α-cholestan-3β-ol	Campestanol
$C_{29}\Delta^{5,22}$	24-ethylcholesta-5,22-dien-3β-ol	Stigmasterol
$C_{29}\Delta^{22}$	24-ethyl-5α-cholesta-22-en-3β-ol	Stigmastanol
$C_{29}\Delta^{5}$	24-ethylcholest-5-en-3β-ol	β-Sitosterol
$C_{29}\Delta^{0}$	24-ethyl-5α-cholestan-3β-ol	β-Sitostanol
$C_{30}\Delta^{22}$	4α,23,24-trimethyl-5α-cholest-22-en-3β-ol	Dinosterol

post-depositional loss) for any downcore sample at depositional time t (sterols$_t$) can be solved using the following equations:

$$k' = 0.86 \times (a_0 + t)^{-1.12} \qquad (2)$$

$$\text{sterols}_{corr} = \text{sterols}_t / [\exp - (k' \times t)] \qquad (3)$$

The sterols$_t$ was initially termed as the sum of several sterols (Canuel and Martens, 1996); however, given almost similar degradation behaviors between individual sterols under anaerobic conditions (Sun and Wakeham, 1994; Canuel and Martens, 1996; Harvey and Macko, 1997; Sun and Wakeham, 1998; Grossi et al., 2001), the sterols$_t$ can be also utilized to calculate sterols$_{corr}$ for each individual sterol. The value of a_0 has been found to be several decades in coastal and shelf areas (Middelburg, 1989; Jia et al., 2013). For simplicity, an empirical 59-year value for a_0 calculated by Jia et al. (2013)

for site A9 outside the PRE (see **Figure 1** for location) was used in this study.

RESULTS

Spatial Distribution of Sterols and Stanols in the Three Cores

A great variety of sterols and stanols were identified in core S401 sediments (**Figure 2**; **Table 2**); however, many of them, especially C_{28} and C_{29} sterols were below detection limit in most samples in cores S101 and S201. Accordingly, the common compounds in three cores, including 4-desmethyl sterols $C_{27}\Delta^{5,22}$, $C_{27}\Delta^{5}$, and $C_{28}\Delta^{5,22}$ and their 5α-stanol counterparts ($C_{27}\Delta^{22}$, $C_{27}\Delta^{0}$, and $C_{28}\Delta^{22}$, respectively), as well as 4-methyl sterol $C_{30}\Delta^{22}$, were
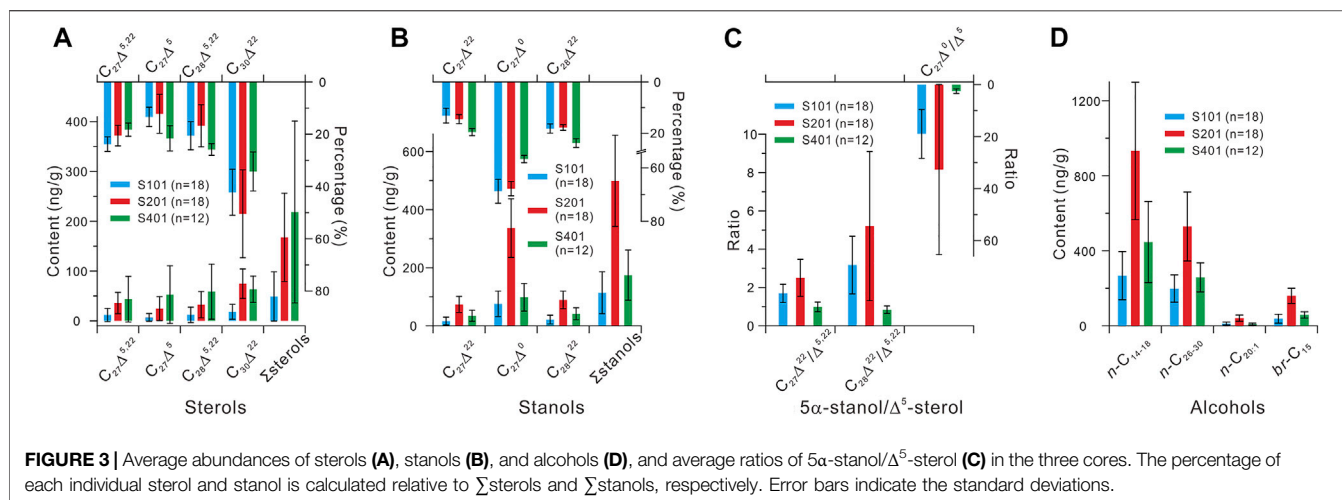
FIGURE 3 | Average abundances of sterols **(A)**, stanols **(B)**, and alcohols **(D)**, and average ratios of 5α-stanol/Δ^5-sterol **(C)** in the three cores. The percentage of each individual sterol and stanol is calculated relative to $\sum$sterols and $\sum$stanols, respectively. Error bars indicate the standard deviations.

preferentially used for comparisons among different cores. The information of other sterol and stanol compounds detected in core S401 (see **Figure 2** and **Table 2**) is also given in **Supplementary Table S1**.

On the whole, contents of $\sum$sterols (i.e., the sum of $C_{27}\Delta^{5,22}$, $C_{27}\Delta^5$, $C_{28}\Delta^{5,22}$, and $C_{30}\Delta^{22}$) were highest (ranged 73–742 ng/g and averaged 219 ± 183 ng/g dry sediment) in core S401 and lowest (ranged 10–189 ng/g and averaged 49 ± 49 ng/g) in core S101 (**Figure 3A**; **Supplementary Table S1**). The sterols exhibited largely similar compositions between cores S101 and S201, with $C_{30}\Delta^{22}$ being the major component (ranged 4–44 and 29–135 ng/g and averaged 18 ± 15 and 75 ± 30 ng/g, and accounted for averaged 42 ± 9% and 50 ± 17% in $\sum$sterols, respectively) followed by $C_{27}\Delta^{5,22}$ (24 ± 3% and 21 ± 4%, respectively), $C_{28}\Delta^{5,22}$ (21 ± 5% and 17 ± 8%, respectively) and minimal $C_{27}\Delta^5$ (13 ± 4% and 12 ± 7%, respectively) (**Figure 3A**; **Supplementary Table S1**). The $C_{30}\Delta^{22}$ was also dominant in core S401 (ranged 28–125 ng/g and averaged 63 ± 26 ng/g, and accounted for averaged 34 ± 7% in $\sum$sterols), followed by relatively equivalent $C_{28}\Delta^{5,22}$ (26 ± 2%), $C_{27}\Delta^5$ (22 ± 5%) and $C_{27}\Delta^{5,22}$ (18 ± 3%) (**Figure 3A**; **Supplementary Table S1**). Moreover, contents of individual sterols and $\sum$sterols exhibited strong positive correlations with each other (**Supplementary Table S2**), thereby allowing for $\sum$sterols to provide a general view of the sterol distribution in the three cores, as shown later.

Contents of $\sum$stanols (i.e., the sum of $C_{27}\Delta^{22}$, $C_{27}\Delta^0$, and $C_{28}\Delta^{22}$) were lowest (ranged 34–240 ng/g and averaged 114 ± 72 ng/g) in core S101 and highest (ranged 272–761 ng/g and averaged 499 ± 157 ng/g) in core S201 (**Figure 3B**; **Supplementary Table S1**). The stanols exhibited largely similar compositions between the three cores, with $C_{27}\Delta^0$ being the major component (ranged 25–153, 187–505, and 40–208 ng/g and averaged 76 ± 44, 336 ± 101, and 98 ± 47 ng/g, and accounted for averaged 69 ± 4%, 68 ± 3%, and 57 ± 1% in $\sum$stanols in cores S101, S201, and S401, respectively) followed by $C_{28}\Delta^{22}$ (18 ± 2%, 18 ± 1% and 24 ± 2%, respectively) and $C_{27}\Delta^{22}$ (13 ± 3%, 14 ± 2%, and 20 ± 1%, respectively) (**Figure 3B**; **Supplementary Table S1**).

The stanols were more abundant than sterol counterparts in cores S101 and S201 (**Figures 3A,B**; **Supplementary Table S1**), yielding relatively high ratio values of $C_{27}\Delta^0/\Delta^5$ (ranged 2.7–33.7 and 4.9–134.6 and averaged 18.6 ± 9.2 and 32.7 ± 32.7, respectively), $C_{28}\Delta^{22}/\Delta^{5,22}$ (ranged 0.7–5.7 and 1.2–13.3 and averaged 3.1 ± 1.5 and 5.2 ± 3.9, respectively), and $C_{27}\Delta^{22}/\Delta^{5,22}$ (ranged 0.7–2.6 and 1.1–4.6 and averaged 1.7 ± 0.5 and 2.5 ± 1.0, respectively) (**Figure 3C**). However, the stanol abundances were slightly higher or even lower than sterol counterparts in core S401 (**Figures 3A,B**; **Supplementary Table S1**), yielding comparatively lower ratio values of $C_{27}\Delta^0/\Delta^5$ (ranged 1.0–3.5 and averaged 2.5 ± 0.9), $C_{28}\Delta^{22}/\Delta^{5,22}$ (ranged 0.4–1.1 and averaged 0.8 ± 0.2), and $C_{27}\Delta^{22}/\Delta^{5,22}$ (ranged 0.5–1.3 and averaged 1.0 ± 0.3) (**Figure 3C**). Furthermore, these three ratio pairs showed strong positive correlations with each other (**Supplementary Table S3**), thereby allowing for $C_{28}\Delta^{22}/\Delta^{5,22}$ to provide a general view of the ratio distribution in the three cores, as shown below.

Temporal Distribution of Sterols and Stanols Over the Past Few Decades

Contents of $\sum$sterols (and individual sterols as demonstrated in **Supplementary Table S2**) displayed roughly similar variation features in cores S101 and S201; i.e., relatively low concentration without significant change before ~1985 (averaged 21 ± 13 and 103 ± 32 ng/g, respectively) followed by large oscillation during ~1985–1995 (varied 19–101–67 and 141–315–70, respectively), and a rapid increase after ~1995 (ranged 67–189 and 70–313 ng/g, respectively) (**Figure 4**). Temporal variation of $\sum$sterols in core S401 exhibited largely similar patterns with cores S101 and S201 before ~1985 and after ~1995 (averaged 148 ± 58 and 431 ± 282 ng/g, respectively); however, the oscillation during ~1985–1995 did not occur in core S401 likely due to low sediment rate and time resolution of the core (two data at the time interval; **Figure 4** and **Table 1**).

Values of the $C_{28}\Delta^{22}/\Delta^{5,22}$ ratio (and other two ratio pairs as demonstrated in **Supplementary Table S3**) oscillated in large amplitudes in cores S101 and S201 (ranged 0.7–5.7 and 1.2–13.3,
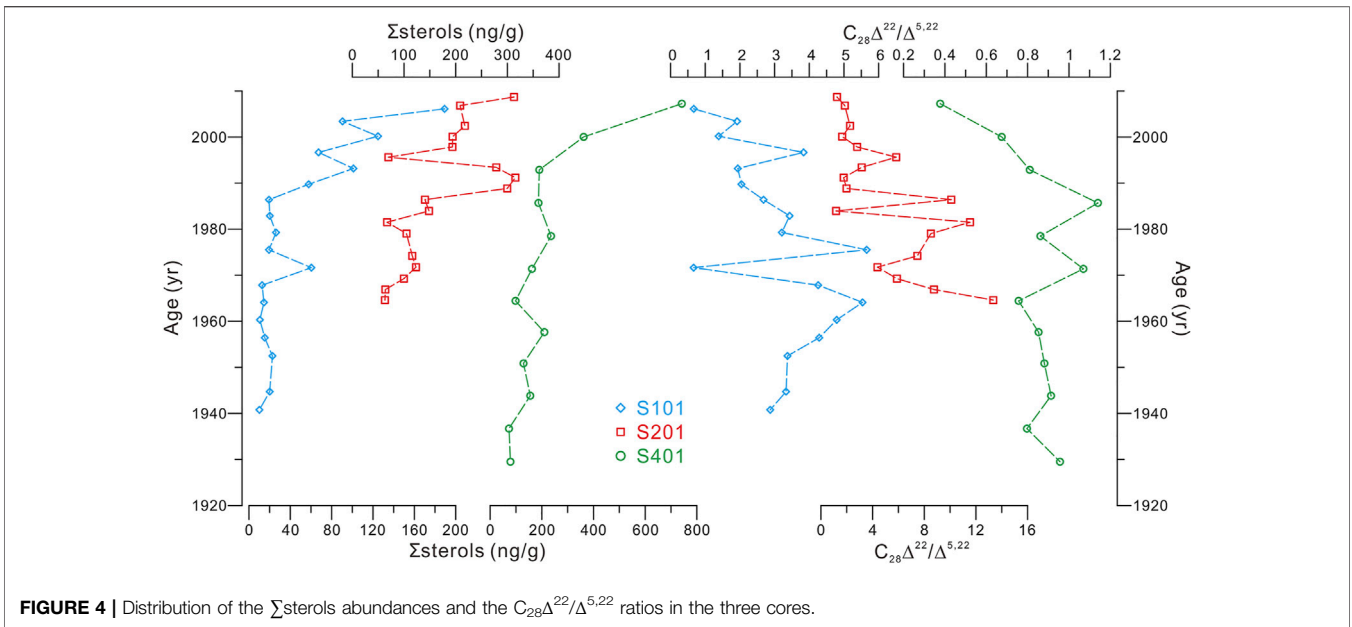
FIGURE 4 | Distribution of the ∑sterols abundances and the $C_{28}\Delta^{22}/\Delta^{5,22}$ ratios in the three cores.
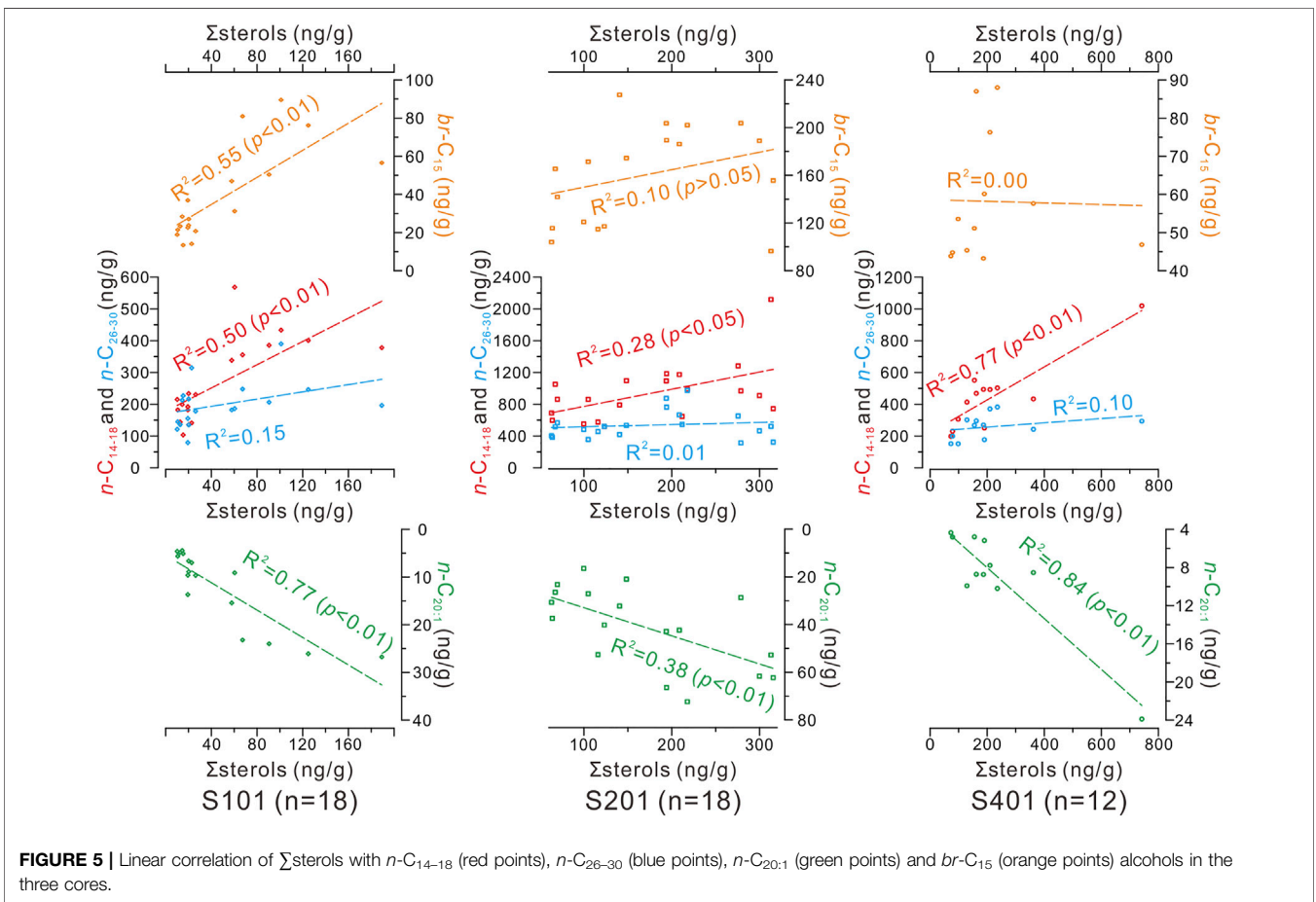
FIGURE 5 | Linear correlation of ∑sterols with n-C_{14-18} (red points), n-C_{26-30} (blue points), n-$C_{20:1}$ (green points) and br-C_{15} (orange points) alcohols in the three cores.

respectively) but swung less variably in core S401 (ranged 0.4–1.1) (**Figure 4**). Distributions of the $C_{28}\Delta^{22}/\Delta^{5,22}$ ratio varied similarly in shape between cores S101 and S201 but changed diversely in terms of multi-year variations as compared to core S401 (**Figure 4**) likely due to the low-resolution data of the core (**Table 1**). Temporal variations of the $C_{28}\Delta^{22}/\Delta^{5,22}$ ratio exhibited no clear trends before ~1980s; after that, however, there occurred a persistent decreasing trend in cores S101 (from 3.2 to 0.7) and S401 (from 1.1 to 0.4) or basically remained at relatively lower values in core S201 (mostly <3 with two exceptions) (**Figure 4**).

Distribution of *n*- and *Br*-Alcohols in the Three Cores

On the whole, contents of n-C_{14-18}, n-C_{26-30} and br-C_{15} alcohols were highest in core S201 (ranged 518–2,118, 313–974, and 96–228 ng/g and averaged 932 ± 366, 530 ± 183, and 160 ± 40 ng/g, respectively) and lowest in core S101 (ranged 103–568, 79–390, and 13–90 ng/g and averaged 268 ± 128, 199 ± 73, and 38 ± 24 ng/g, respectively) (**Figure 3D**; **Supplementary Table S4**). The n-$C_{20:1}$ alcohol was also most abundant in core S201 (ranged 16–72 ng/g and averaged 41 ± 17 ng/g) but was least abundant in core S401 (ranged 4–24 ng/g and averaged 9 ± 5 ng/g) (**Figure 3D**; **Supplementary Table S4**).

Moreover, contents of n-C_{14-18} and n-$C_{20:1}$ alcohols exhibited strong positive correlations with ∑sterols (and individual sterols as demonstrated in **Supplementary Table S2**) in the three cores (**Figure 5**). The abundances of br-C_{15} alcohols resembled to the n-alcohol ratios of C_{15-17}/C_{16-20} down the cores (**Supplementary Figure S1**) but correlated insignificantly with ∑sterols (and individual sterols as demonstrated in **Supplementary Table S2**) especially in cores S201 and S401 (**Figure 5**).

DISCUSSION

### Origin of Sterols and Their Application as Primary Production (PP)

The biological sources of the $C_{27}\Delta^{5,22}$, $C_{27}\Delta^{5}$, $C_{28}\Delta^{5,22}$, and $C_{30}\Delta^{22}$ sterols in the study area are likely predominantly marine organisms. This is supported by the better correlations of ∑sterols (and individual sterols as demonstrated in **Supplementary Table S2**) with marine-sourced n-C_{14-18} alcohols than with terrigenous-originated n-C_{26-30} alcohols in the three cores (**Figure 5**). Presently, it is difficult to constrain the species-specific sources of these biological sterols, owing to their ubiquity in a wide range of marine organisms, including phytoplankton and zooplankton (Volkman, 1986; Volkman et al., 1998; Volkman, 2003; Rampen et al., 2010), which are abundant in the study area (Wang et al., 2011; Duan et al., 2014; Ren et al., 2020). However, the strong correlations among these sterols in the three cores (**Supplementary Table S2**) suggest common factors in modulating production of various phytoplankton and subsequent consumption by zooplankton in food chains. This is further supported by the strong

correlations between ∑sterols (and individual sterols as demonstrated in **Supplementary Table S2**) and n-$C_{20:1}$ alcohol (**Figure 5**), a diagnostic biomarker for copepods (Kattner and Krause, 1989), which dominate zooplankton composition in the YDU area (Ren et al., 2020). Therefore, here, ∑sterols, the sum of sterols produced by various phytoplankton (i.e., diatoms and dinoflagellates) and/or phytoplankton-dependent zooplankton, rather than individual sterol, are more suitable to roughly indicate PP in the study area. Nevertheless, the ∑sterols loss due to degradation processes in the water column and/or sediments (e.g., Sun and Wakeham, 1994; Canuel and Martens, 1996; Prahl et al., 2000; Sinninghe Damsté et al., 2002; Wakeham et al., 2002; Hernández-Sánchez et al., 2014) may confound ∑sterols burial fluxes to reflect initial export PP.

Present-day investigations in the YDU area reveal that total phytoplankton abundances are not highly variable at various depths of the upper 30-m water column (i.e., 78.9×10^2 unit in surface water vs. 50.7×10^2 unit at 20- to 30-m water depth; Wang et al., 2011). This occurrence should be due to that the photic zone (i.e., 0–30 m) can extend readily to the seafloor of the study sites (water depths <35 m; **Table 1**). Phytoplankton-derived lipid biomarkers could undergo least degradation in such shallow water depths, as even in deep-sea water columns, including the Arabian Sea (0–3,380 m; Prahl et al., 2000; Wakeham et al., 2002) and the South East Atlantic Ocean (0–100 m; Hernández-Sánchez et al., 2014), the loss of biomarkers (including sterols) has been found insignificant. Accordingly, the application of buried ∑sterols to infer paleo-PP in the YDU area is feasible as long as degradation in sediments is properly considered.

Thus, we used a model proposed by Canuel and Martens (1996) to estimate the degradation loss of ∑sterols in sediments and further to assess its influence on the downcore changes of ∑sterols, similar with the approach for organic carbon-degradation correction applied in the PRE (Jia et al., 2013) using the (Middelburg, 1989) model. It should be noted that the (Canuel and Martens, 1996) model is established for the anoxic environments of Cape Lookout Bight but is also likely applicable for coastal areas where aerobic conditions are usually confined to uppermost few-millimeter sediments (e.g., Hansen and Blackburn, 1991; Sun and Wakeham, 1994; Sun and Wakeham, 1998; Arndt et al., 2013). As illustrated in **Figure 6**, the initial ∑sterols (∑sterols$_{corr}$) changed almost similarly with the burial ∑sterols, indicating that downcore ∑sterols can be used to infer PP variations in the study area, despite the degradation loss could be as high as ~24% in sediment depths.

According to **Figure 4**, the ∑sterols with largely similar variation features in most parts of the three cores suggest common factors controlling PP in the YDU area over the past few decades. The change in abundances of algal sterols, which is associated with PP variability, has been also documented offshore the PRE (i.e., at site A9; **Figure 1**) over the past century (Jia et al., 2013), demonstrating, again, the reliability of burial ∑sterols to reflect export PP in the coastal northern SCS. Moreover, the variability of PP offshore the PRE is considered as a result from
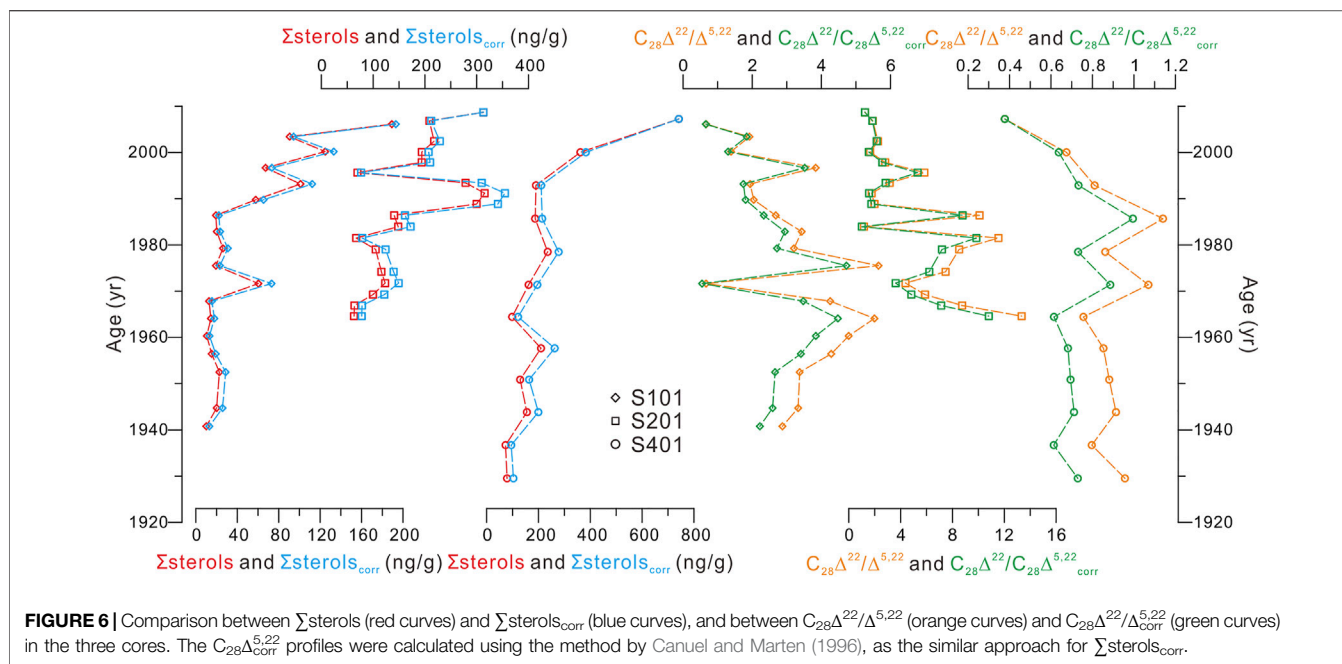
FIGURE 6 | Comparison between ∑sterols (red curves) and ∑sterols$_{corr}$ (blue curves), and between $C_{28}\Delta^{22}/\Delta^{5,22}$ (orange curves) and $C_{28}\Delta^{22}/\Delta^{5,22}_{corr}$ (green curves) in the three cores. The $C_{28}\Delta^{5,22}_{corr}$ profiles were calculated using the method by Canuel and Marten (1996), as the similar approach for ∑sterols$_{corr}$.

the fluvial nutrient influx from the Pearl River (Jia et al., 2013). However, riverine nutrient inputs could be largely ruled out as a cause for PP variations in the study area due to minor influence of the Pearl River plume, as have been described in detail in our previous study (Zhu et al., 2018). This is further supported by the relatively lower sterol abundances in core S101 than in cores S201 and S401 (**Figure 3A**; **Supplementary Table S1**), because core S101 was located closest to, whereas the other two cores were distributed further away from, the PRE (**Figure 1**). Our previous study on long chain diols derived DI-2 records in three cores revealed that the increasing trend in the upwelling intensity with inter-annual variability is a common phenomenon covering the YDU area over recent decades (Zhu et al., 2018). Thus, we deem that the upwelling-induced nutrients may have exerted an important effect on the variations of PP and sterol abundances at the sites.

Origin of Stanols

The diatom community is almost the exclusively dominant algae in the study area, accounting for ~88% of the total phytoplankton composition with *Proboscia alata* being the major species, followed by *T. nitzschioides*, *Pseudo-nitzschia pungens*, and *S. costatum* (Wang et al., 2011). The *S. costatum* is predominantly abundant in the PRE (Qiu et al., 2010; Shen et al., 2011); however, $C_{28}\Delta^{24(28)}$ that can be produced *in vivo* by *S. costatum* (Barrett et al., 1995; Rampen et al., 2010) has not been identified (or reported) in this region (Hu et al., 2009; Strong et al., 2012; Strong et al., 2013; Jia et al., 2013; Guo et al., 2019). The $C_{28}\Delta^{24(28)}$ was not detected either in core S101 (closest to the PRE), suggesting that $C_{28}\Delta^{24(28)}$ would be little produced by algae (i.e., *S. costatum*) in the coastal northern SCS. However, $C_{28}\Delta^{24(28)}$ was identified, despite with minimal amounts (averaged 7 ± 4 ng/g; **Supplementary Table S1**) in core S401 (farthest to the PRE),

thus indicating that anaerobic conversion of $C_{28}\Delta^{5,24(28)}$ is more likely responsible for the presence of $C_{28}\Delta^{24(28)}$ at the site. The contribution of *T. nitzschioide* to $C_{27}\Delta^{22}$ (Barrett et al., 1995; Rampen et al., 2010) in the three cores, however, could not be completely neglected based on the present study.

Dinoflagellates, despite account for a minute fraction of the total phytoplankton community, are the second most abundant algae in the YDU area (Wang et al., 2011; Duan et al., 2014). The dominance of *Scrippsiella* sp. in dinoflagellate floras in the study area (Duan et al., 2014) likely suggests this species as a considerable contributor to $C_{27}\Delta^{0}$. This is further supported by the much high values of the $C_{27}\Delta^{0}/\Delta^{5}$ ratio; i.e., an average of 32.7 in core S201 (**Figure 3C**), as such a similarly high $C_{27}\Delta^{0}/\Delta^{5}$ ratio has been also documented in *Scrippsiella* sp. (Mansour et al., 1999). The possibility of dinoflagellate *G. sanguineum* as a biological source for $C_{28}\Delta^{22}$ (Mansour et al., 1999), however, could be largely ruled out, owing to the absence of this species in the YDU area (Wang et al., 2011; Duan et al., 2014). Similarly, some other marine organisms that have been reported to contain considerable fractional abundances of $C_{28}\Delta^{22}$ (Volkman et al., 1990; Nelson et al., 2000; Nelson et al., 2001) have also not been observed (or reported) in the study area (Wang et al., 2011; Duan et al., 2014; Ren et al., 2020).

Implication of the $C_{28}\Delta^{22}/\Delta^{5,22}$ Ratio for Bottom Water DO Condition

As explained above, the $C_{27}\Delta^{22}/\Delta^{5,22}$ and $C_{27}\Delta^{0}/\Delta^{5}$ ratios are not suitable as reliable indicators for anaerobic transformation processes at the study sites, as *T. nitzschioide* and *Scrippsiella* sp. may contribute to $C_{27}\Delta^{22}$ and $C_{27}\Delta^{0}$, respectively. In contrast, the insignificant contribution of living organisms to other 5α-stanols (i.e., $C_{28}\Delta^{24(28)}$ and $C_{28}\Delta^{22}$) suggests they are more likely
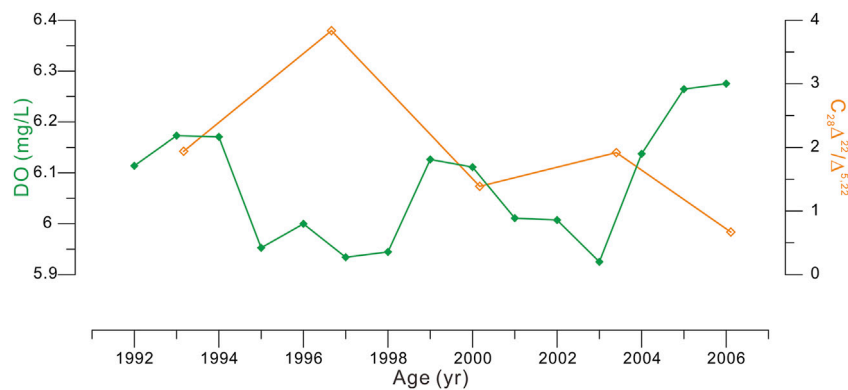
FIGURE 7 | Comparison of the $C_{28}\Delta^{22}/\Delta^{5,22}$ ratios (orange curve) in core S101 with bottom water DO concentrations (4-year running average; green curve) at proximate station MM13 (**Figure 1**) during 1991–2007. The annual mean DO concentration is estimated from monthly data collected by the Environmental Protection Department, Hong Kong (https://cd.epic.epd.gov.hk/EPICRIVER/marine). Note that monitoring DO data are available since the early 1990s, so given time span (before 2006) and resolution (averaged 3.6 years per 2-cm interval) in core S101 (**Table 1**), this figure shows a rough comparison between records of the $C_{28}\Delta^{22}/\Delta^{5,22}$ ratio and monitoring DO content (4-year running average) during 1991–2007.

derived from the anaerobic conversion of their Δ^5-sterol counterparts. The $C_{28}\Delta^{22}/\Delta^{5,22}$ ratio is selected in this study because the three cores all contained detailed data of this ratio. However, another confounding factor should be ruled out before the application of the ratio as a redox indicator, i.e., the $C_{28}\Delta^{22}/\Delta^{5,22}$ ratio variations down the cores could be caused by differential degradation, given that 5α-stanols are more refractory than their respective Δ^5-sterol counterparts (e.g., Nishimura and Koyama, 1977; Wakeham, 1989; Arzayus and Canuel, 2004; Bogus et al., 2012). Lines of evidence have revealed that biomarker (including sterols) degradation is insignificant even in deep-sea water columns as compared to in sediments (e.g., Prahl et al., 2000; Sinninghe Damsté et al., 2002; Wakeham et al., 2002; Hernández-Sánchez et al., 2014). Therefore, the potential loss of $C_{28}\Delta^{5,22}$ in the studied shallow water column (<35 m; **Table 1**) is not considered, but instead, its loss in sediments were evaluated. Here, we used the model by Canuel and Martens (1996) to estimate the initial $C_{28}\Delta^{5,22}$ ($C_{28}\Delta_{corr}^{5,22}$, as the case for $\sum sterols_{corr}$) and then assessed the potential influence of degradation process on the downcore $C_{28}\Delta^{22}/\Delta^{5,22}$ variations. As illustrated in **Figure 6**, profiles of the corrected $C_{28}\Delta^{22}/\Delta^{5,22}$ ($C_{28}\Delta^{22}/C_{28}\Delta_{corr}^{5,22}$) followed those of buried $C_{28}\Delta^{22}/\Delta^{5,22}$ in three cores, indicating that degradation loss of $C_{28}\Delta^{5,22}$ in sediment depths is not responsible for the downcore changes in the $C_{28}\Delta^{22}/\Delta^{5,22}$ ratios.

Therefore, by elimination, we deem the anaerobic conversion of $C_{28}\Delta^{5,22}$ is a more reasonable process to interpret past $C_{28}\Delta^{22}/\Delta^{5,22}$ variations. Previous studies have revealed that the 5α-stanol/Δ^5-sterol ratios increase sharply in the oxic-anoxic transition zone in waters (Wakeham, 1989; Wakeham et al., 2007; Berndmeyer et al., 2014; Wakeham, 2020) and sediments (Nishimura and Koyama, 1977). Conditions in such a zone are well suited to the development of a large and most active microbial population (Karl, 1978; Larock et al., 1979; Lin et al., 2008; Rodriguez-Mora et al., 2013; Berndmeyer et al., 2014). In the YDU area, the significant reduction of $C_{28}\Delta^{5,22}$ in the water column could be largely ruled out due to the

absence of anaerobic waters (and thus oxic-anoxic transition zone), as revealed by monitoring records (Zhang et al., 2018; **Figure 7**) and satellite observations (the World Ocean Atlas 2018; https://www.nodc.noaa.gov/cgi-bin/OC5/SELECT/woaselect.pl?parameter=3).

Thus, we believe the anaerobic conversion of $C_{28}\Delta^{5,22}$ should have occurred principally in sediments. The hydrogenation reduction of Δ^5-steros has been found to be rapid in the oxic-anoxic transition zone in microbiologically active sediments in the early sedimentation process, below which the hydrogenation rate is greatly attenuated (Nishimura and Koyama, 1977). This scenario may thus suggest that, in the coastal YDU, the greater part of $C_{28}\Delta^{22}$ originating from the hydrogenation of $C_{28}\Delta^{5,22}$ may have been produced mainly in the microbiologically active oxic-anoxic transition zone, which would lie in surface sediments. This is because 1) aerobic conditions are usually confined to the uppermost few-millimeter layer in coastal areas (e.g., Hansen and Blackburn, 1991; Sun and Wakeham, 1994; Sun and Wakeham, 1998; Arndt et al., 2013) and 2) microbial population is highest near the sediment surface and drops off steeply with depths in coastal marine sediments (e.g., Jørgensen and Revsbech, 1989; Sahm et al., 1999; Arndt et al., 2013). Moreover, comparison of surface sediments (≤2 cm) from different lakes with diverse bottom water redox potentials demonstrates an increasing trend in the 5α-stanol/Δ^5-sterol ratios from relatively oxidizing (i.e., 0.36 at Lake Kizaki) to reducing (i.e., 0.66 at Lake Suigetsu) environments (Nishimura and Koyama, 1977). Similarly, the 5α-stanol/Δ^5-sterol ratios are found higher in surface sediments with comparatively lower bottom water DO levels in the Yangtze River estuary (Zhu et al., 2012) and the PRE (Guo, 2015), implying that the ratio records in downcore sediments may reflect bottom water (surface sediment) redox conditions in the past. This is followed by a recent study on short cores around Penguin Island, demonstrating that sedimentary variations of the 5α-stanol/Δ^5-sterol ratios may be attributed to changes in bottom water conditions at the study sites at the time of deposition (Ceschim et al., 2016).

Accordingly, in this study, sedimentary $C_{28}\Delta^{22}/\Delta^{5,22}$ ratios are likely also predominantly determined by bottom water DO conditions that modulate the extent of anaerobic conversion of $C_{28}\Delta^{5,22}$ at its initial deposition as a component of surface sediments. Here, DO condition is not an either–or concept between anaerobic and aerobic but a description of likely continuous change in DO concentration, although a common quantitative relation between the $C_{28}\Delta^{22}/\Delta^{5,22}$ ratio and DO concentration cannot be made at present and could be site specific. This is because the so-called anaerobic conversion has been found to take place under various redox conditions not strictly devoid of oxygen with a reported wide range of DO concentrations from 0 to ~10.6 mg/L (Wakeham, 1989; Wakeham, 2020; Wakeham et al., 2007; Berndmeyer et al., 2014; Guo, 2015). This implies that in the YDU area the anaerobic conversion of $C_{28}\Delta^{5,22}$ may occur persistently and with varying degrees in surface sediments in response to variable bottom water DO concentrations. Given that the mean temporal resolutions of the three cores were ~2–7 years per 2-cm sediment interval (**Table 1**), the $C_{28}\Delta^{22}/\Delta^{5,22}$ ratio in each sediment interval is effectively a result of multi-year accumulated anaerobic conversion processes. Such an integrated continuous accumulation record would dampen or smooth out greater variations on shorter time scales (e.g., monthly and seasonal) and thereby should tend to reflect longer-term (i.e., multi-year) mean state of DO conditions. This point is supported by previous studies showing that the 5α-stanol/Δ^5-sterol ratios are not reflective of seasonal-biased DO signals in surface sediments, where bottom water experience dramatically seasonal DO variability (Nishimura and Koyama, 1977; Zhu et al., 2012; Guo, 2015), implying that seasonal DO dynamics is hard to be recorded in sedimentary $C_{28}\Delta^{22}/\Delta^{5,22}$ ratios. Therefore, we believe multi-year mean state of bottom water DO conditions should be responsible for sedimentary $C_{28}\Delta^{22}/\Delta^{5,22}$ records in the study area. This is consistent with a rough comparison between the $C_{28}\Delta^{22}/\Delta^{5,22}$ ratios in core S101 (3.6 years per 2-cm sedimentary interval; **Table 1**) and 4-year averaged bottom water DO variations at proximal monitoring station MM13 (**Figure 1**) during 1991–2007, showing higher $C_{28}\Delta^{22}/\Delta^{5,22}$ ratio values corresponding with lower DO concentrations (**Figure 7**). According to the ratio records down the three cores (**Figure 4**), DO concentrations varied at each site but similarly in shape between sites S101 and S201 with no clear temporal trend before ~1980s; after that, DO concentrations increased gradually (i.e., at sites S101 and S401) or shifted to a relatively abundant state (i.e., at site S201).

## Potential Factors on Bottom Water DO Variations

Our novel sterol data (**Figure 3A**; **Supplementary Table S1**), together with already published diol data (Zhu et al., 2018), reinforce that the Pearl River plume contributes insignificantly to the study area, consistent with a recent study suggesting the influence of runoff from the Pearl River only within a certain range (Xu et al., 2020). Therefore, the input from the Pearl River is not considered as the most important driver on bottom water

DO dynamics, but instead, the climate-induced upwelling-involved physical-biogeochemical processes (i.e., source water, wind stress, oceanic warming, photosynthetic production, and aerobic consumption) should be important to influence past changes in bottom water DO concentrations in the YDU area. These upwelling-involved processes have also been proposed as potentially important drivers on bottom water DO dynamics in many other upwelling regions without direct riverine influence (e.g., Fennel and Testa, 2019 and references therein).

The substantial impact of upwelling intensity on DO condition has been observed in upwelling regions off Peru, showing overall enhanced oxygenation in response to gradually intensified upwelling, which is attributed to a subtle oxygenation trend in the upwelled source waters (Cardich et al., 2019). The advection of upwelled source waters has been also proposed as a dominant factor controlling DO variability in many other upwelling regions (e.g., Grantham et al., 2004; Monteiro et al., 2006; Monteiro et al., 2008; Chan et al., 2008; Mohrholz et al., 2008). However, a 29-year observation across the northern SCS shelf area during 1976–2004 reveals a significant decrease in DO concentrations at various depths of the upper 200-m water column (Ning et al., 2009), thus likely transporting reduced-oxygenated source waters from outer shelf to inner coastal area at times of upwelling over recent decades. This scenario would rather decrease bottom water oxygenation and thus promote the anaerobic conversion of $C_{28}\Delta^{5,22}$ in more reducing surface sediments, leading to elevated $C_{28}\Delta^{22}/\Delta^{5,22}$ ratios in recent decades that is in contrast with our present records. Therefore, the physical supply of source waters from outer shelf due to upwelling activity is not likely the major cause for bottom water DO variability in the study area.

Increases in southwesterly wind stress have been simulated to decrease bottom water hypoxia by eroding vertical stratification and aerating deep waters in the PRE (Wei et al., 2016; Lu et al., 2018). However, a time-series (2001–2015) observation in the nearby Mirs Bay reveals that larger hypoxic areas in bottom waters are often observed during years with longer-lasting southwesterly wind as a result of enhanced stratification, extended residence time of bottom waters, and onshore transport of low-oxygenated source waters induced by stable upwelling (Zhang et al., 2018). This inconsistency between the two proximal regions just to the west of YDU suggests that the actual impact of local southwesterly wind on DO condition may be highly site specific in the coastal northern SCS. Specific to our study sites, the wind stress appears to exert a minor effect on bottom water DO condition, as the $C_{28}\Delta^{22}/\Delta^{5,22}$ ratio correlated insignificantly with DI-2 inferred local wind stress in the three cores (**Supplementary Figure S2**).

Oceanic warming has a high potential to enhance stratification, decrease the DO solubility, and increase the rate of organic matter mineralization, thus eventually increasing oxygen deficiency and causing low-oxygen condition in bottom waters (Ning et al., 2009; Keeling et al., 2010; Schmidtko et al., 2017; Breitburg et al., 2018; Fennel and Testa, 2019). However, the important role of oceanic warming in regulating bottom water DO condition could be largely ruled out in the study area, because the $C_{28}\Delta^{22}/\Delta^{5,22}$ ratio changed
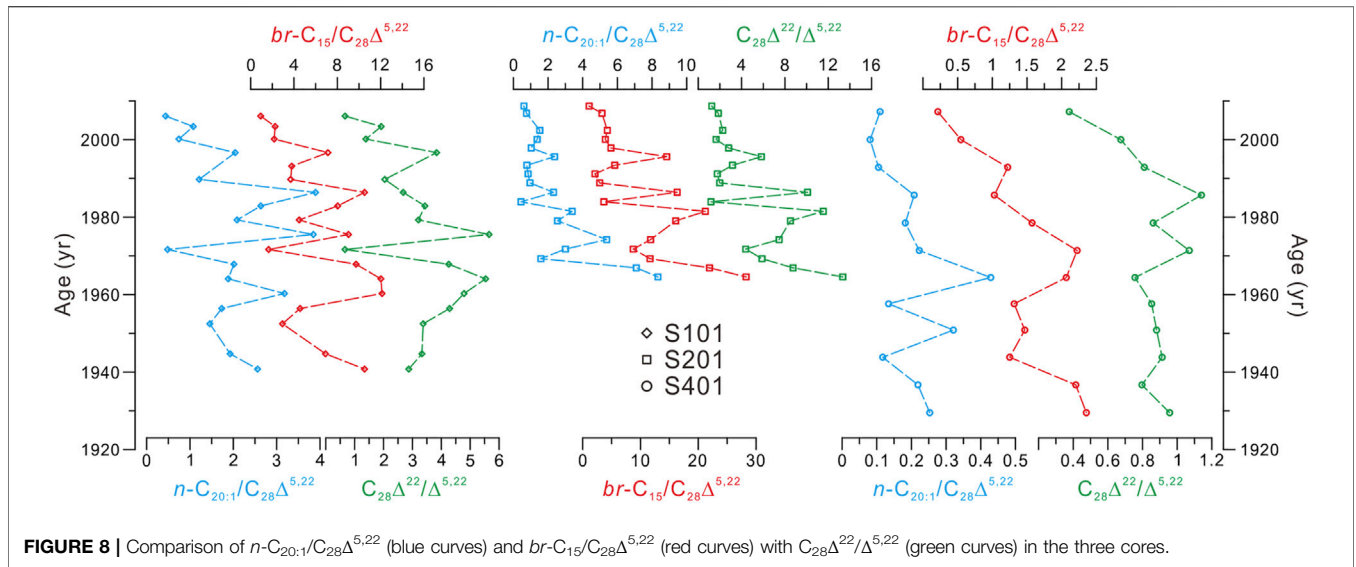
FIGURE 8 | Comparison of n-$C_{20:1}$/$C_{28}\Delta^{5,22}$ (blue curves) and br-C_{15}/$C_{28}\Delta^{5,22}$ (red curves) with $C_{28}\Delta^{22}$/$\Delta^{5,22}$ (green curves) in the three cores.
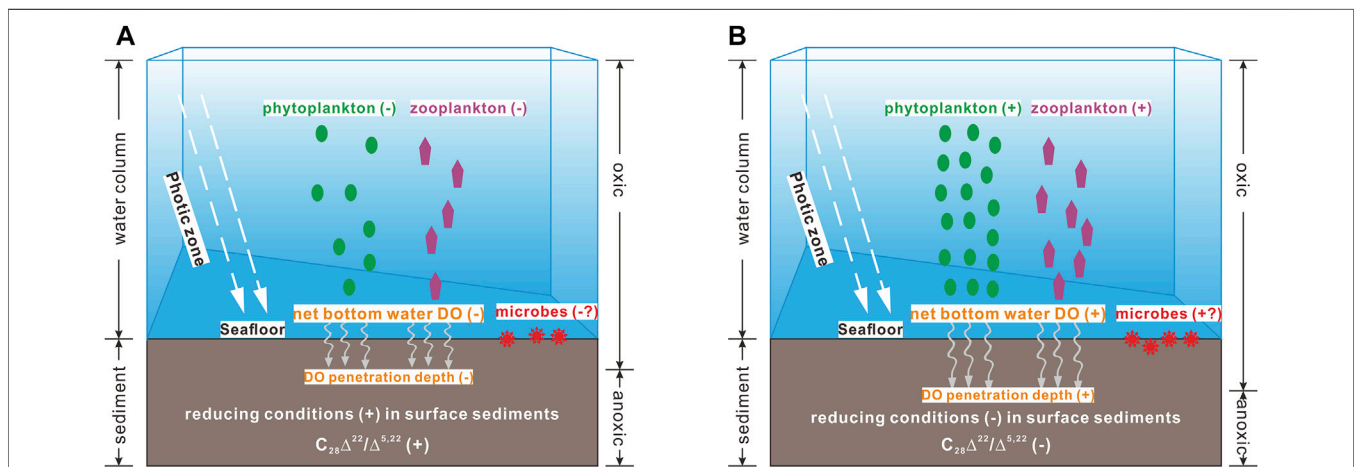
FIGURE 9 | Schematic diagram of the biogeochemical mechanism of photosynthetic production in determining bottom water DO variations in surface sediments in the shallow, clear YDU area, showing **(A)** decreased bottom water oxygenation (–) and more reducing surface sediment (+) indicated by higher $C_{28}\Delta^{22}$/$\Delta^{5,22}$ ratio (+) in response to lower PP indicated by less abundant ∑sterols (–), and **(B)** increased bottom water oxygenation (+) and less reducing surface sediment (–) indicated by lower $C_{28}\Delta^{22}$/$\Delta^{5,22}$ ratio (–) in response to higher PP indicated by more abundant ∑sterols (+). Here, anaerobic conversion of $C_{28}\Delta^{5,22}$ is setting to occur principally in the oxic-anoxic transition zone in microbiologically active surface sediment, and thus, the $C_{28}\Delta^{22}$/$\Delta^{5,22}$ ratio at each sedimentary interval is mainly governed by bottom water DO level at the time of deposition. For detail in, e.g., figure **(B)**, higher abundances of phytoplankton can fuel more abundant zooplankton (**Figure 5**) in the total photic water column; however, higher amounts of phytoplankton (and phytoplankton-dependent zooplankton) derived relatively labile organic matter may not always lead to increased microbial biomass (i.e., at sites S201 and S401; **Figure 5**). Regardless of certain degree of DO consumption by zooplankton respiration and microbial remineralization, the dominant role of DO production by phytoplankton photosynthesis in the photic zone (**Figure 8**) may still lead to higher extent of net bottom water DO penetrating into surface sediment, resulting in less reducing condition and thus lower sedimentary $C_{28}\Delta^{22}$/$\Delta^{5,22}$ ratio.

uncorrelated with LDI-derived annual mean SST in three cores (**Supplementary Figure S2**). Similar findings suggesting less importance of oceanic warming on DO condition in the coastal area than in the open ocean have been also made in other studies (e.g., Breitburg et al., 2018; Fennel and Testa, 2019 and references therein).

The above difficulties in the interpretation on the $C_{28}\Delta^{22}$/$\Delta^{5,22}$ ratio-inferred bottom water DO variability prompt us to consider the possible role of biogeochemical processes, because we notice

that the $C_{28}\Delta^{22}$/$\Delta^{5,22}$ ratios correlate substantially reversed with the ∑sterols abundances in three cores (**Figure 4**). This occurrence suggests that bottom water DO concentrations change positively with total PP in the YDU area, which is compatible with recent studies focused on a small area of the western YDU, showing that low-oxygen areas do not coincide with the regions of high PP (Wei et al., 2016; Zhang et al., 2018). This phenomenon may be related with the competitive results of the twofold impacts induced by elevated PP in shallow, clear

waters (Fennel and Testa, 2019); i.e., exacerbated oxygen depletion due to high rate of respiration and mineralization, and sufficient oxygen supply through photosynthetic production. To give a rough assessment of the competitive results between the biogeochemical oxygen sink and source, we compared the records of zooplankton and microbes (consumers) with records of phytoplankton (producers). As illustrated in **Figure 8**, distributions of the $n\text{-}C_{20:1}/C_{28}\Delta^{5,22}$ and $br\text{-}C_{15}/C_{28}\Delta^{5,22}$ ratios, indicative of the relative abundances of zooplankton and microbes compared with phytoplankton, respectively, changed almost in parallel with the $C_{28}\Delta^{22}/\Delta^{5,22}$ ratios in the three cores. These occurrences suggest that, in our studied shallow-water area with less turbidity due to minor influence of the Pearl River plume (Zhu et al., 2018; this study), the oxygen production *via* photosynthesis may have exceeded biological oxygen consumption by zooplankton respiration and microbial remineralization, leading to a strong positive relationship between water column PP and bottom water (surface sediment) DO (**Figure 4**). **Figure 9** illustrates general scenarios of the dominant role of photosynthetic production in the photic water column (i.e., 0–30 m; Wang et al., 2011) just above the seafloor of the study sites (water depths <35 m; **Table 1**) in determining bottom water redox conditions in surface sediments. We suggest that net photosynthetic oxygen production outweighs upwelling-involved source water– and oceanic warming–induced deoxygenation in bottom waters in the YDU area. We believe this phenomenon may also occur elsewhere with similar coastal upwelling conditions, such as shallow, clear waters with minor influence of riverine terrigenous input. However, the dominance of biogeochemical forcing on bottom water DO condition may be greatly attenuated in large river-impacted upwelling regions. For example, in the Mirs Bay (**Figure 1**) that is the western boundary of YDU affected by the Pearl River plume, the physical processes (i.e., freshwater discharge), rather than biogeochemical dynamics, are proposed as the most important drivers for inter-annual bottom water DO variability (Zhang et al., 2018).

CONCLUSION

A series of sterols and stanols were identified, and the 5α-stanol/Δ^5-sterol ratios were examined for their applicability for redox reconstruction in sediment cores in the YDU area in the coastal northern SCS. The ∑sterols abundances with roughly similar variation features were observed in most parts of the three cores, suggesting common factors controlling PP, which may be related to upwelling-induced nutrients over the past few decades. The $C_{27}\Delta^{22}/\Delta^{5,22}$ and $C_{27}\Delta^0/\Delta^5$ ratios were not so reliable to reflect redox conditions because marine organism may produce these two stanols *in vivo*. However, some other ratio pairs such as the $C_{28}\Delta^{22}/\Delta^{5,22}$ ratio can be accepted as a feasible redox indicator to infer changes of redox conditions in surface sediments, which are largely dependent on bottom water DO levels. The

$C_{28}\Delta^{22}/\Delta^{5,22}$ ratio records in three cores showed oscillations in varying degrees and exhibited no clear trends in bottom water DO concentrations before ~1980s but indicated a persistent increasing trend in oxygenation (at sites S101 and S401) or basically shifted to relatively higher DO level (at site S201) since then. This occurrence could be caused by the changes in net ecosystem production, as indicated by the $n\text{-}C_{20:1}/C_{28}\Delta^{5,22}$ and $br\text{-}C_{15}/C_{28}\Delta^{5,22}$ records that changed similarly with the $C_{28}\Delta^{22}/\Delta^{5,22}$ records in the three cores. This study may provide a perspective on the responses of bottom water DO variation to upwelling and climate change in the future in shallow, clear coastal upwelling regions.

DATA AVAILABILITY STATEMENT

The original contributions presented in the study are included in the article/**Supplementary Material**; further inquiries can be directed to the corresponding author.

AUTHOR CONTRIBUTIONS

GJ conceived and supervised the entire work and commented on the paper. XZ performed the experiments, analyzed the data, and wrote the article. YT and AM prepared the figures. WX, LM, SX, and WY contributed to the discussion and writing of this paper.

SUPPLEMENTARY MATERIAL

The Supplementary Material for this article can be found online at: https://www.frontiersin.org/articles/10.3389/feart.2021.759317/full#supplementary-material

REFERENCES

Arndt, S., Jorgensen, B. B., LaRowe, D. E., Middelburg, J. J., Pancost, R. D., and Regnier, P. (2013). Quantifying the Degradation of Organic Matter in marine Sediments: A Review and Synthesis. *Earth-Science Rev.* 123, 53–86. doi:10.1016/j.earscirev.2013.02.008

Arzayus, K. M., and Canuel, E. A. (2005). Organic Matter Degradation in Sediments of the York River Estuary: Effects of Biological vs. Physical Mixing. *Geochimica et Cosmochimica Acta* 69 (2), 455–464. doi:10.1016/j.gca.2004.06.029

Bakun, A. (1990). Global Climate Change and Intensification of Coastal Ocean Upwelling. *Science* 247 (4939), 198–201. doi:10.1126/science.247.4939.198

Barrett, S. M., Volkman, J. K., Dunstan, G. A., and Leroi, J.-M. (1995). Sterols of 14 Species of Marine Diatoms (Bacillariophyta)1. *J. Phycol* 31 (3), 360–369. doi:10.1111/j.0022-3646.1995.00360.x

Berndmeyer, C., Thiel, V., Schmale, O., Wasmund, N., and Blumenberg, M. (2014). Biomarkers in the Stratified Water Column of the Landsort Deep (Baltic Sea). *Biogeosciences* 11 (23), 7009–7023. doi:10.5194/bg-11-7009-2014

Bogus, K. A., Zonneveld, K. A. F., Fischer, D., Kasten, S., Bohrmann, G., and Versteegh, G. J. M. (2012). The Effect of Meter-Scale Lateral Oxygen Gradients at the Sediment-Water Interface on Selected Organic Matter Based Alteration, Productivity and Temperature Proxies. *Biogeosciences* 9 (4), 1553–1570. doi:10.5194/bg-9-1553-2012

Breitburg, D., Levin, L. A., Oschlies, A., Grégoire, M., Chavez, F. P., Conley, D. J., et al. (2018). Declining Oxygen in the Global Ocean and Coastal Waters. *Science* 359 (6371), eaam7240. doi:10.1126/science.aam7240

Breitburg, D. L., Hondorp, D. W., Davias, L. A., and Diaz, R. J. (2009). Hypoxia, Nitrogen, and Fisheries: Integrating Effects across Local and Global Landscapes. *Annu. Rev. Mar. Sci.* 1, 329–349. doi:10.1146/annurev.marine.010908.163754

Canuel, E. A., and Martens, C. S. (1996). Reactivity of Recently Deposited Organic Matter: Degradation of Lipid Compounds Near the Sediment-Water Interface. *Geochimica et Cosmochimica Acta* 60 (10), 1793–1806. doi:10.1016/0016-7037(96)00045-2

Cardich, J., Sifeddine, A., Salvatteci, R., Romero, D., Briceno-Zuluaga, F., Graco, M., et al. (2019). Multidecadal Changes in marine Subsurface Oxygenation off central Peru during the Last Ca. 170 Years. *Front. Mar. Sci.* 6, 16. doi:10.3389/fmars.2019.00270

Ceschim, L. M. M., Dauner, A. L. L., Montone, R. C., Figueira, R. C. L., and Martins, C. C. (2016). Depositional History of Sedimentary Sterols Around Penguin Island, Antarctica. *Antarctic Sci.* 28 (6), 443–454. doi:10.1017/s0954102016000274

Chan, F., Barth, J. A., Lubchenco, J., Kirincich, A., Weeks, H., Peterson, W. T., et al. (2008). Emergence of Anoxia in the California Current Large marine Ecosystem. *Science* 319 (5865), 920. doi:10.1126/science.1149016

Deutsch, C., Berelson, W., Thunell, R., Weber, T., Tems, C., McManus, J., et al. (2014). Centennial Changes in North Pacific Anoxia Linked to Tropical Trade Winds. *Science* 345 (6197), 665–668. doi:10.1126/science.1252332

Diaz, R. J., and Rosenberg, R. (2008). Spreading Dead Zones and Consequences for marine Ecosystems. *Science* 321 (5891), 926–929. doi:10.1126/science.1156401

Dong, L., Su, J., Ah Wong, L., Cao, Z., and Chen, J.-C. (2004). Seasonal Variation and Dynamics of the Pearl River Plume. *Continental Shelf Res.* 24 (16), 1761–1777. doi:10.1016/j.csr.2004.06.006

Duan, M., Li, H., and Yan, Y. (2014). Community Structure and Seasonal Variation of Phytoplankton in Jieshi Bay and its Adjacent Waters. *Ecologic Sci.* 33 (5), 865–871. doi:10.14108/j.cnki.1008-8873.2014.05.007

Fennel, K., and Testa, J. M. (2019). Biogeochemical Controls on Coastal Hypoxia. *Annu. Rev. Mar. Sci.* 11, 105–130. doi:10.1146/annurev-marine-010318-095138

Gaskell, S. J., and Eglinton, G. (1975). Rapid Hydrogenation of Sterols in a Contemporary Lacustrine Sediment. *Nature* 254 (5497), 209–211. doi:10.1038/254209b0

Grantham, B. A., Chan, F., Nielsen, K. J., Fox, D. S., Barth, J. A., Huyer, A., et al. (2004). Upwelling-driven Nearshore Hypoxia Signals Ecosystem and Oceanographic Changes in the Northeast Pacific. *Nature* 429 (6993), 749–754. doi:10.1038/nature02605

Grossi, V., Blokker, P., and Sinninghe Damsté, J. S. (2001). Anaerobic Biodegradation of Lipids of the marine Microalga *Nannochloropsis salina*. *Org. Geochem.* 32 (6), 795–808. doi:10.1016/s0146-6380(01)00040-7

Guo, W., Jia, G., Ye, F., Xiao, H., and Zhang, Z. (2019). Lipid Biomarkers in Suspended Particulate Matter and Surface Sediments in the Pearl River Estuary, a Subtropical Estuary in Southern China. *Sci. Total Environ.* 646, 416–426. doi:10.1016/j.scitotenv.2018.07.159

Guo, W. (2015). *Source and Biogeochemical Properties of Oragnic Carbon in Water Column and Sediments of Pearl River Estuary*. Beijing, China: University of Chinese Academy of Sciences, 1–146. Availableat: http://d.wanfangdata.com.cn/thesis/Y3054230.

Gutiérrez, D., Bouloubassi, I., Sifeddine, A., Purca, S., Goubanova, K., Graco, M., et al. (2011). Coastal Cooling and Increased Productivity in the Main Upwelling Zone off Peru since the Mid-twentieth century. *Geophys. Res. Lett.* 38, a–n. doi:10.1029/2010gl046324

Hansen, L., and Blackburn, T. (1991). Aerobic and Anaerobic Mineralization of Organic Material in marine Sediment Microcosms. *Mar. Ecol. Prog. Ser.* 75 (2-3), 283–291. doi:10.3354/meps075283

Harvey, H. R., and Macko, S. A. (1997). Kinetics of Phytoplankton Decay during Simulated Sedimentation: Changes in Lipids under Oxic and Anoxic Conditions. *Org. Geochem.* 27 (3-4), 129–140. doi:10.1016/s0146-6380(97)00077-6

Hernández-Sánchez, M. T., LaRowe, D. E., Deng, F., Homoky, W. B., Browning, T. J., Martin, P., et al. (2014). Further Insights into How Sediment Redox Status Controls the Preservation and Composition of Sedimentary Biomarkers. *Org. Geochem.* 76, 220–234. doi:10.1016/j.orggeochem.2014.08.006

Hu, J., Peng, P. a., and Chivas, A. R. (2009). Molecular Biomarker Evidence of Origins and Transport of Organic Matter in Sediments of the Pearl River Estuary and Adjacent South China Sea. *Appl. Geochem.* 24 (9), 1666–1676. doi:10.1016/j.apgeochem.2009.04.035

Hu, J., and Wang, X. H. (2016). Progress on Upwelling Studies in the China Seas. *Rev. Geophys.* 54 (3), 653–673. doi:10.1002/2015rg000505

Huang, X., Meyers, P. A., Jia, C., Zheng, M., Xue, J., Wang, X., et al. (2013). Paleotemperature Variability in central China during the Last 13 Ka Recorded by a Novel Microbial Lipid Proxy in the Dajiuhu Peat deposit. *The Holocene* 23 (8), 1123–1129. doi:10.1177/0959683613483617

Jacobel, A. W., Anderson, R. F., Jaccard, S. L., McManus, J. F., Pavia, F. J., and Winckler, G. (2020). Deep Pacific Storage of Respired Carbon during the Last Ice Age: Perspectives from Bottom Water Oxygen Reconstructions. *Quat. Sci. Rev.* 230, 106065. doi:10.1016/j.quascirev.2019.106065

Jia, G., Xu, S., Chen, W., Lei, F., Bai, Y., and Huh, C.-A. (2013). 100-year Ecosystem History Elucidated from Inner Shelf Sediments off the Pearl River Estuary, China. *Mar. Chem.* 151, 47–55. doi:10.1016/j.marchem.2013.02.005

Jilan, S. (2004). Overview of the South China Sea Circulation and its Influence on the Coastal Physical Oceanography outside the Pearl River Estuary. *Continental Shelf Res.* 24 (16), 1745–1760. doi:10.1016/j.csr.2004.06.005

Jing, Z., Qi, Y., and Du, Y. (2011). Upwelling in the continental Shelf of Northern South China Sea Associated with 1997-1998 El Nino. *J. Geophys. Res.* 116, C02033. doi:10.1029/2010jc006598

Jorgensen, B. B., and Revsbech, N. P. (1989). Oxygen Uptake, Bacterial Distribution, and Carbon-Nitrogen-Sulfur Cycling in Sediments from the baltic Sea - North Sea Transition. *Ophelia* 31 (1), 29–49. doi:10.1080/00785326.1989.10430849

Karl, D. M. (1978). Distribution, Abundance, and Metabolic States of Microorganisms in the Water Column and Sediments of the Black Sea1. *Limnol. Oceanogr.* 23 (5), 936–949. doi:10.4319/lo.1978.23.5.0936

Kattner, G., and Krause, M. (1989). Seasonal Variations of Lipids (Wax Esters, Fatty Acids and Alcohols) in Calanoid Copepods from the North Sea. *Mar. Chem.* 26 (3), 261–275. doi:10.1016/0304-4203(89)90007-8

Keeling, R. F., Kortzinger, A., and Gruber, N. (2010). Ocean Deoxygenation in a Warming World. *Annu. Rev. Mar. Sci.* 2, 199–229. doi:10.1146/annurev.marine.010908.163855

Larock, P. A., Lauer, R. D., Schwarz, J. R., Watanabe, K. K., and Wiesenburg, D. A. (1979). Microbial Biomass and Activity Distribution in an Anoxic, Hypersaline basin. *Appl. Environ. Microbiol.* 37 (3), 466–470. doi:10.1128/aem.37.3.466-470.1979

Levin, L. A., and Breitburg, D. L. (2015). Linking Coasts and Seas to Address Ocean Deoxygenation. *Nat. Clim Change* 5 (5), 401–403. doi:10.1038/nclimate2595

Li, G., Rashid, H., Zhong, L., Xu, X., Yan, W., and Chen, Z. (2018). Changes in Deep Water Oxygenation of the South China Sea since the Last Glacial Period. *Geophys. Res. Lett.* 45 (17), 9058–9066. doi:10.1029/2018gl078568

Lin, X., Scranton, M. I., Chistosodov, A. Y., Varela, R., and Taylor, G. T. (2008). Spatiotemporal Dynamics of Bacterial Populations in the Anoxic Cariaco Basin. *Limnol. Oceanogr.* 53 (1), 37–51. doi:10.4319/lo.2008.53.1.0037

Lu, Z., Gan, J., Dai, M., Liu, H., and Zhao, X. (2018). Joint Effects of Extrinsic Biophysical Fluxes and Intrinsic Hydrodynamics on the Formation of Hypoxia West off the Pearl River Estuary. *J. Geophys. Res. Oceans* 123 (9), 6241–6259. doi:10.1029/2018jc014199

Mansour, M. P., Volkman, J. K., Jackson, A. E., and Blackburn, S. I. (1999). The Fatty Acid and Sterol Composition of Five marine Dinoflagellates. *J. Phycol* 35 (4), 710–720. doi:10.1046/j.1529-8817.1999.3540710.x

Middelburg, J. J. (1989). A Simple Rate Model for Organic Matter Decomposition in marine Sediments. *Geochimica et Cosmochimica Acta* 53 (7), 1577–1581. doi:10.1016/0016-7037(89)90239-1

Mohrholz, V., Bartholomae, C. H., van der Plas, A. K., and Lass, H. U. (2008). The Seasonal Variability of the Northern Benguela Undercurrent and its Relation to the Oxygen Budget on the Shelf. *Continental Shelf Res.* 28 (3), 424–441. doi:10.1016/j.csr.2007.10.001

Monteiro, P. M. S., van der Plas, A. K., Mélice, J.-L., and Florenchie, P. (2008). Interannual Hypoxia Variability in a Coastal Upwelling System: Ocean-Shelf Exchange, Climate and Ecosystem-State Implications. *Deep Sea Res. Oceanographic Res. Pap.* 55 (4), 435–450. doi:10.1016/j.dsr.2007.12.010

Monteiro, P. M. S., van der Plas, A., Mohrholz, V., Mabille, E., Pascall, A., and Joubert, W. (2006). Variability of Natural Hypoxia and Methane in a Coastal Upwelling System: Oceanic Physics or Shelf Biology? *Geophys. Res. Lett.* 33 (16), 5. doi:10.1029/2006gl026234

Mudge, S. M., and Norris, G. E. (1997). Lipid Biomarkers in the Conwy Estuary (North Wales, UK): A Comparison between Fatty Alcohols and Sterols. *Mar. Chem.* 57 (1-2), 61–84. doi:10.1016/s0304-4203(97)00010-8

Naafs, B. D. A., Inglis, G. N., Blewett, J., McClymont, E. L., Lauretano, V., Xie, S., et al. (2019). The Potential of Biomarker Proxies to Trace Climate, Vegetation, and Biogeochemical Processes in Peat: A Review. *Glob. Planet. Change* 179, 57–79. doi:10.1016/j.gloplacha.2019.05.006

Nakakuni, M., Dairiki, C., Kaur, G., and Yamamoto, S. (2017). Stanol to Sterol Ratios in Late Quaternary Sediments from Southern California: An Indicator for Continuous Variability of the Oxygen Minimum Zone. *Org. Geochem.* 111, 126–135. doi:10.1016/j.orggeochem.2017.06.009

Nakakuni, M., Kitano, J., Uemura, H., and Yamamoto, S. (2018). Modern Sediment Records of Stanol to Sterol Ratios in Lake Suigetsu, Japan: An Indicator of Variable Lacustrine Redox Conditions. *Org. Geochem.* 119, 59–71. doi:10.1016/j.orggeochem.2018.02.004

Nelson, M. M., Mooney, B. D., Nichols, P. D., and Phleger, C. F. (2001). Lipids of Antarctic Ocean Amphipods: Food Chain Interactions and the Occurrence of Novel Biomarkers. *Mar. Chem.* 73 (1), 53–64. doi:10.1016/s0304-4203(00)00072-4

Nelson, M. M., Phleger, C. F., Mooney, B. D., and Nichols, P. D. (2000). Lipids of Gelatinous Antarctic Zooplankton: Cnidaria and Ctenophora. *Lipids* 35 (5), 551–559. doi:10.1007/s11745-000-555-5

Ning, X., Lin, C., Hao, Q., Liu, C., Le, F., and Shi, J. (2009). Long Term Changes in the Ecosystem in the Northern South China Sea during 1976-2004. *Biogeosciences* 6 (10), 2227–2243. doi:10.5194/bg-6-2227-2009

Nishimura, M., and Koyama, T. (1977). The Occurrence of Stanols in Various Living Organisms and the Behavior of Sterols in Contemporary Sediments. *Geochimica et Cosmochimica Acta* 41 (3), 379–385. doi:10.1016/0016-7037(77)90265-4

Prahl, F. G., Dymond, J., and Sparrow, M. A. (2000). Annual Biomarker Record for export Production in the central Arabian Sea. *Deep-Sea Res. Part II-Topical Stud. Oceanography* 47 (7-8), 1581–1604. doi:10.1016/s0967-0645(99)00155-1

Qiu, D., Huang, L., Zhang, J., and Lin, S. (2010). Phytoplankton Dynamics in and Near the Highly Eutrophic Pearl River Estuary, South China Sea. *Continental Shelf Res.* 30 (2), 177–186. doi:10.1016/j.csr.2009.10.015

Rampen, S. W., Abbas, B. A., Schouten, S., and Sinninghe Damsté, J. S. (2010). A Comprehensive Study of Sterols in marine Diatoms (Bacillariophyta): Implications for Their Use as Tracers for Diatom Productivity. *Limnol. Oceanogr.* 55 (1), 91–105. doi:10.4319/lo.2010.55.1.0091

Ren, Y., Ke, Z., Tan, Y., and Li, K. (2020). Community Structure of Zooplankton and its Influencing Factors in the Eastern Waters of Nan'ao Island, Guangdong. *J. Trop. Oceanography* 39 (2), 65–76. doi:10.11978/2019051

Rodriguez-Mora, M. J., Scranton, M. I., Taylor, G. T., and Chistoserdov, A. Y. (2013). Bacterial Community Composition in a Large marine Anoxic basin: a Cariaco Basin Time-Series Survey. *FEMS Microbiol. Ecol.* 84 (3), 625–639. doi:10.1111/1574-6941.12094

Sahm, K., MacGregor, B. J., Jorgensen, B. B., and Stahl, D. A. (1999). Sulphate Reduction and Vertical Distribution of Sulphate-Reducing Bacteria Quantified by rRNA Slot-Blot Hybridization in a Coastal marine Sediment. *Environ. Microbiol.* 1 (1), 65–74. doi:10.1046/j.1462-2920.1999.00007.x

Schmidtko, S., Stramma, L., and Visbeck, M. (2017). Decline in Global Oceanic Oxygen Content during the Past Five Decades. *Nature* 542 (7641), 335–339. doi:10.1038/nature21399

Shen, P.-P., Li, G., Huang, L.-M., Zhang, J.-L., and Tan, Y.-H. (2011). Spatio-temporal Variability of Phytoplankton Assemblages in the Pearl River Estuary, with Special Reference to the Influence of Turbidity and Temperature. *Continental Shelf Res.* 31 (16), 1672–1681. doi:10.1016/j.csr.2011.07.002

Sinninghe Damsté, J. S., Rijpstra, W. I. C., and Reichart, G.-j. (2002). The Influence of Oxic Degradation on the Sedimentary Biomarker Record II. Evidence from Arabian Sea Sediments. *Geochimica et Cosmochimica Acta* 66 (15), 2737–2754. doi:10.1016/s0016-7037(02)00865-7

Strong, D., Flecker, R., Valdes, P. J., Wilkinson, I. P., Rees, J. G., Michaelides, K., et al. (2013). A New Regional, Mid-holocene Palaeoprecipitation Signal of the Asian Summer Monsoon. *Quat. Sci. Rev.* 78, 65–76. doi:10.1016/j.quascirev.2013.07.034

Strong, D. J., Flecker, R., Valdes, P. J., Wilkinson, I. P., Rees, J. G., Zong, Y. Q., et al. (2012). Organic Matter Distribution in the Modern Sediments of the Pearl River Estuary. *Org. Geochem.* 49, 68–82. doi:10.1016/j.orggeochem.2012.04.011

Sun, M.-Y., and Wakeham, S. G. (1998). A Study of Oxic/anoxic Effects on Degradation of Sterols at the Simulated Sediment-Water Interface of Coastal Sediments. *Org. Geochem.* 28 (12), 773–784. doi:10.1016/s0146-6380(98)00043-6

Sun, M.-Y., and Wakeham, S. G. (1994). Molecular Evidence for Degradation and Preservation of Organic Matter in the Anoxic Black Sea Basin. *Geochimica et Cosmochimica Acta* 58 (16), 3395–3406. doi:10.1016/0016-7037(94)90094-9

Sydeman, W. J., García-Reyes, M., Schoeman, D. S., Rykaczewski, R. R., Thompson, S. A., Black, B. A., et al. (2014). Climate Change and Wind Intensification in Coastal Upwelling Ecosystems. *Science* 345 (6192), 77–80. doi:10.1126/science.1251635

Treignier, C., Derenne, S., and Saliot, A. (2006). Terrestrial and marine *N*-Alcohol Inputs and Degradation Processes Relating to a Sudden Turbidity Current in the Zaire canyon. *Org. Geochem.* 37 (9), 1170–1184. doi:10.1016/j.orggeochem.2006.03.010

Volkman, J. K. (1986). A Review of Sterol Markers for marine and Terrigenous Organic Matter. *Org. Geochem.* 9 (2), 83–99. doi:10.1016/0146-6380(86)90089-6

Volkman, J. K., Barrett, S. M., Blackburn, S. I., Mansour, M. P., Sikes, E. L., and Gelin, F. (1998). Microalgal Biomarkers: A Review of Recent Research Developments. *Org. Geochem.* 29 (5-7), 1163–1179. doi:10.1016/s0146-6380(98)00062-x

Volkman, J. K., Kearney, P., and Jeffrey, S. W. (1990). A New Source of 4-methyl Sterols and 5α(H)-stanols in Sediments: Prymnesiophyte Microalgae of the Genus Pavlova. *Org. Geochem.* 15 (5), 489–497. doi:10.1016/0146-6380(90)90094-g

Volkman, J. (2003). Sterols in Microorganisms. *Appl. Microbiol. Biotechnol.* 60 (5), 495–506. doi:10.1007/s00253-002-1172-8

Wakeham, S. G., Amann, R., Freeman, K. H., Hopmans, E. C., Jørgensen, B. B., Putnam, I. F., et al. (2007). Microbial Ecology of the Stratified Water Column of the Black Sea as Revealed by a Comprehensive Biomarker Study. *Org. Geochem.* 38 (12), 2070–2097. doi:10.1016/j.orggeochem.2007.08.003

Wakeham, S. G. (2020). Organic Biogeochemistry in the Oxygen-Deficient Ocean: A Review. *Org. Geochem.* 149, 104096. doi:10.1016/j.orggeochem.2020.104096

Wakeham, S. G., Peterson, M. L., Hedges, J. I., and Lee, C. (2002). Lipid Biomarker Fluxes in the Arabian Sea, with a Comparison to the Equatorial Pacific Ocean. *Deep Sea Res. Part Topical Stud. Oceanography* 49 (12), 2265–2301. doi:10.1016/s0967-0645(02)00037-1

Wakeham, S. G. (1989). Reduction of Stenols to Stanols in Particulate Matter at Oxic-Anoxic Boundaries in Sea Water. *Nature* 342 (6251), 787–790. doi:10.1038/342787a0

Wang, D., Gouhier, T. C., Menge, B. A., and Ganguly, A. R. (2015). Intensification and Spatial Homogenization of Coastal Upwelling under Climate Change. *Nature* 518 (7539), 390–394. doi:10.1038/nature14235

Wang, Y., Lin, M., Lin, G. M., and Xiang, P. (2011). Community Composition of Phytoplankton in Fujian-Guangdong Coastal Upwelling Region in Summer and Related Affecting Factors. *Ying Yong Sheng Tai Xue Bao* 22 (2), 503–512. Availableat: http://www.cjae.net/CN/Y2011/V22/I02/503.

Watson, A. J. (2016). Oceans on the Edge of Anoxia. *Science* 354 (6319), 1529–1530. doi:10.1126/science.aaj2321

Wei, X., Zhan, H., Ni, P., and Cai, S. (2016). A Model Study of the Effects of River Discharges and Winds on Hypoxia in Summer in the Pearl River Estuary. *Mar. Pollut. Bull.* 113 (1-2), 414–427. doi:10.1016/j.marpolbul.2016.10.042

Xu, S., Zhang, Z., Jia, G., Yu, K., Lei, F., and Zhu, X. (2020). Controlling Factors and Environmental Significance of BIT and δ13C of Sedimentary GDGTs from the Pearl River Estuary, China over Recent Decades. *Estuarine, Coastal Shelf Sci.* 233, 106534. doi:10.1016/j.ecss.2019.106534

Yang, H., Ding, W., and Xie, S. (2014). Distribution of Microbial Fatty Acids and Fatty Alcohols in Soils from an Altitude Transect of Mt. Jianfengling in Hainan, China: Implication for Paleoaltimetry and Paleotemperature Reconstruction. *Sci. China Earth Sci.* 57 (5), 999–1012. doi:10.1007/s11430-013-4729-8

Zhang, H., Cheng, W., Chen, Y., Yu, L., and Gong, W. (2018). Controls on the Interannual Variability of Hypoxia in a Subtropical Embayment and its Adjacent Waters in the Guangdong Coastal Upwelling System, Northern South China Sea. *Ocean Dyn.* 68 (8), 923–938. doi:10.1007/s10236-018-1168-2

Zhu, C., Pan, J.-M., and Pancost, R. D. (2012). Anthropogenic Pollution and Oxygen Depletion in the Lower Yangtze River as Revealed by Sedimentary Biomarkers. *Org. Geochem.* 53, 95–98. doi:10.1016/j.orggeochem.2012.09.008

Zhu, X., Jia, G., Mao, S., and Yan, W. (2018). Sediment Records of Long Chain Alkyl Diols in an Upwelling Area of the Coastal Northern South China Sea. *Org. Geochem.* 121, 1–9. doi:10.1016/j.orggeochem.2018.03.014

Conflict of Interest: The authors declare that the research was conducted in the absence of any commercial or financial relationships that could be construed as a potential conflict of interest.

Publisher's Note: All claims expressed in this article are solely those of the authors and do not necessarily represent those of their affiliated organizations or those of the publisher, the editors, and the reviewers. Any product that may be evaluated in this article, or claim that may be made by its manufacturer, is not guaranteed or endorsed by the publisher.